# Meta-analytic connectivity and behavioral parcellation of the human cerebellum

Michael C. Riedel [a], Kimberly L. Ray [b], Anthony S. Dick [c], Matthew T. Sutherland [c], Zachary Hernandez [d], P. Mickle Fox [a], Simon B. Eickhoff [e,f], Peter T. Fox [a,g,h], Angela R. Laird [i,*]

[a] Research Imaging Institute, University of Texas Health Science Center, San Antonio, TX, USA
[b] Imaging Research Center, University of California Davis, Sacramento, CA, USA
[c] Department of Psychology, Florida International University, Miami, FL, USA
[d] Department of Electrical and Computer Engineering, University of Houston, Houston, TX, USA
[e] Institute of Neuroscience and Medicine (INM-1), Research Centre Jülich, Jülich, Germany
[f] Institute for Clinical Neuroscience and Medical Psychology, Heinrich-Heine University, Dusseldorf, Germany
[g] South Texas Veterans Health Care System, San Antonio, TX, USA
[h] State Key Laboratory for Brain and Cognitive Sciences, University of Hong Kong, Hong Kong, China
[i] Department of Physics, Florida International University, Miami, FL, USA

### ARTICLE INFO

### ABSTRACT

The cerebellum historically has been thought to mediate motor and sensory signals between the body and cerebral cortex, yet cerebellar lesions are also associated with altered cognitive behavioral performance. Neuroimaging evidence indicates that the cerebellum contributes to a wide range of cognitive, perceptual, and motor functions. Here, we used the BrainMap database to investigate whole-brain co-activation patterns between cerebellar structures and regions of the cerebral cortex, as well as associations with behavioral tasks. Hierarchical clustering was performed to meta-analytically identify cerebellar structures with similar cortical co-activation, and independently, with similar correlations to specific behavioral tasks. Strong correspondences were observed in these separate but parallel analyses of meta-analytic connectivity and behavioral metadata. We recovered differential zones of cerebellar co-activation that are reflected across the literature. Furthermore, the behaviors and tasks associated with the different cerebellar zones provide insight into the specialized function of the cerebellum, relating to high-order cognition, emotion, perception, interoception, and action. Taken together, these task-based meta-analytic results implicate distinct zones of the cerebellum as critically involved in the monitoring and mediation of psychological responses to internal and external stimuli.

Published by Elsevier Inc.

## Introduction

Functional neuroimaging has made significant progress toward advancing our understanding of the human cerebellum, yet a comprehensive understanding of this important structure remains a challenge. The cerebellum has long been assumed to act within the sensorimotor system and so its functions have been assumed to contribute to sensation and movement. Historically, this was based largely on studies of sensorimotor impairments following cerebellar lesions or atrophy, including impairments in coordination (Zwicker et al., 2011), eye movement (Miall et al., 2001), articulation (Wise et al., 1999), swallowing (Suzuki et al., 2003), tremor (Greco et al., 2002), or gait (the ataxia syndromes; Schmahmann, 2004). The anatomical connectivity of the cerebellum, which receives afferents from the spinal cord (Schweighofer et al., 1998), with the motor cortex (Chen, 2004) supports the region's significant involvement in motor functions. However, anatomical connectivity also suggests the cerebellum's association with non-motor, higher-level cognitive and affective functions. For example, tract-tracing studies in the macaque monkey have identified cortico–ponto–cerebellar connections originating from regions of the cortex associated with language, spatial, executive function, and affective processing (Middleton and Strick, 1994; Schmahmann and Caplan, 2006; Schmahmann and Pandya, 1989; Schmahmann and Sherman, 1998; Schmahmann et al., 1999; Stoodley, 2011).

Further evidence for the cerebellum's involvement in higher-level cognition comes from clinical findings. Specifically, localized cerebellar lesions lead to: 1) disturbances of executive function/cognitive control (e.g., planning, set-shifting, reasoning, working memory); 2) impaired visual–spatial processing and memory; 3) personality changes (e.g., flat affect and disinhibited/inappropriate behavior); and 4) disruptions of language and speech, including verbal fluency, dysprosodia,

* Corresponding author at: Department of Physics, Florida International University, Modesto Maidique Campus, AHC-4 310, 11200 SW 8th Street, Miami, FL 33199, USA. Fax: +1 305 348 6700.
E-mail address: alaird@fiu.edu (A.R. Laird).

agrammatism and anomia (Schmahmann and Sherman, 1998). This specific neurophysiological profile following confined cerebellar lesions has been classified under the rubric of cerebellar–cognitive–affective syndrome (Schmahmann and Sherman, 1998; Schmahmann, 2004).

In addition to and consistent with these clinical findings, emerging neuroimaging evidence also has identified cerebellar contributions during the execution of cognitive and affective tasks (Schmahmann, 1991; Schmahmann and Sherman, 1998; Salmi et al., 2009; Stoodley et al., 2011, 2012; Strata et al., 2011). In a meta-analysis of 53 studies, Stoodley et al. (2009) demonstrated cerebellar activation during sensorimotor integration, language, spatial processing, verbal working memory, cognitive control, and emotional processing. Evidence from multiple studies also indicates that this diverse range of cerebellar functions relies on a broadly distributed system of cortical connections. That is, the cerebellum exhibits significant functional connectivity (FC) with frontal, parietal, temporal, and occipital cortices during resting-state and task-based functional neuroimaging studies (Allen et al., 2005; Buckner et al., 2011; Dobromyslin et al., 2012; Habas et al., 2009; Krienen and Buckner, 2009; O'Reilly et al., 2010; Sang et al., 2012). The combined results of these experiments provide a preliminary framework for understanding the complexities of cortico–cerebellar connectivity and associated relations with cognition.

Despite the rapid increase in functional neuroimaging investigations, interpretations of cerebellar FC patterns and the accompanying behavioral implications has progressed more slowly. Large-scale meta-analytic methods now provide processing tools and heuristic frameworks to objectively assess convergent patterns of brain activity associated with specific behavioral domains. In particular, meta-analytic connectivity modeling (MACM) is used to comprehensively identify whole-brain co-activation patterns consistently reported across a number of published neuroimaging studies. This method has been employed to enhance understanding of the FC of the amygdala (Robinson et al., 2009), parietal operculum (Eickhoff et al., 2009) and regions of the default-mode network (Laird et al., 2009a, 2009b), and can be flexibly applied to the characterization of other brain regions. Although MACM previously has been utilized to investigate cerebellar co-activation, prior work has relied on defining regions of interest either by morphometric abnormalities (Reetz et al., 2012) or by aggregating across regions of a probabilistic atlas (Balsters et al., 2014). In accordance with literature reviews supporting differential cortical connectivity with distinct cerebellar zones, Balsters et al. (2014) investigated the preferential co-activation of a group of cerebellar structures contributing to motor performance, and a group of structures contributing to cognition. Their results demonstrated that a group of superior cerebellum structures exhibited preferential co-activation with the motor cortex, whereas a group of inferior cerebellar lobules demonstrated co-activation with prefrontal regions. Furthermore, Stoodley et al. (2009) modeled whole-brain co-activation profiles to demonstrate that separate behavioral domains were represented differently across the cerebellum. While these previous studies have provided new insight into the heterogeneous FC profile of the cerebellum, they were based on specific a priori hypotheses about cerebellar function and limited in that regions of interest were *subjectively* chosen. In contrast, the present study investigated both the large-scale meta-analytic connectivity and behavioral properties of the cerebellum through independent meta-analyses without assumptions regarding cerebellar behavior or functional organization.

Harnessing the accumulated volume of published neuroimaging results on the cerebellum, we sought to address two questions. First, is there a dissociable organization of connectivity within subregions of the cerebellum that can be observed employing meta-analytic tools? Second, can such FC architecture clarify the diverse behavioral functions that have been ascribed to the cerebellum? To address these questions, we performed a series of independent yet parallel meta-analyses (i.e., co-activation and behavioral) in the BrainMap environment using cerebellar regions of interest (ROIs) defined according to a probabilistic anatomical atlas (Diedrichsen et al., 2009). Resultant co-activation and behavioral profiles were examined to characterize meta-analytic congruency across these two parcellation schemes.

## Materials and methods

### Structural parcellation of the cerebellum

To investigate cerebellar functional organization, a reliable parcellation strategy is first needed. The most widely accepted current structural parcellation of the cerebellum is a normalized probabilistic atlas consisting of 28 structures (Diedrichsen et al., 2009) (Fig. 1) based on the Schmahmann cerebellum parcellation strategy (Schmahmann et al., 2000). This atlas has been used in various ways including confirmation and comparison of anatomical connectivity patterns (Rosch et al., 2010), identification of structural contributions across diverse tasks (Vahdat et al., 2011; Wu et al., 2011; Wildenberg et al., 2011; Moulton et al., 2011), examination of differential cortico–cerebellar co-activation (Balsters et al., 2014) and the longitudinal investigation of cerebellar morphometry (Tiemeier et al., 2010). Images delineating the volume of each cerebellar structure were obtained according to the Diedrichsen parcellation strategy in MNI space (http://www.icn.ucl.ac.uk/motorcontrol/imaging/propatlas.htm), with left and right structures treated independently (Diedrichsen et al., 2009). One structure (VIIa Crus I Vermis) occupying less than 0.1% of the total volume of the cerebellum was omitted from further analysis. The remaining 27 structures were seeded in the BrainMap database to identify functional experiments in which other brain areas were observed to co-activate with each of the cerebellar ROIs.

### Co-activation meta-analyses

#### Meta-analytic connectivity modeling (MACM)

The first step in developing a functional organization of the cerebellum was to generate whole-brain co-activation profiles for each cerebellar ROI. We used the *Sleuth* software application (www.brainmap.org/sleuth) to search the BrainMap database for all experiments that reported one or more activation coordinates within a binarized mask for each of the 27 cerebellar ROIs analyzed. The number of coordinates reported in each structure (Table 1, *Metadata Foci*) indicates the strength of each region's representation within the database. We then downloaded whole-brain coordinates of regions which were simultaneously coactive with the coordinates observed in the cerebellar ROIs. Search results were limited to activation coordinates (not deactivations) reported in studies involving only healthy subjects. We converted coordinates reported in Talairach into MNI space (Lancaster et al., 2007; Laird et al., 2010). In addition to whole-brain co-activation coordinates, we also downloaded the corresponding metadata from the BrainMap taxonomy (Fox et al., 2005; Laird and Turner, 2012), which catalogues the experimental design, stimulus type (e.g., *Heat*, *Numbers*, *Objects*), paradigm class (e.g., *Face Monitor/Discrimination*, *Theory of Mind*), and behavioral domain (e.g., *Action*, *Emotion.Sadness*) of each study.

Once the whole-brain co-activation coordinates were identified for each of the cerebellar ROIs, we performed meta-analytic connectivity modeling (MACM) using *GingerALE* (www.brainmap.org/ale) (Laird et al., 2009a, 2009b; Robinson et al., 2009; Eickhoff et al., 2009). We derived a MACM image representing the above-chance probability that a given voxel co-activated with the cerebellar ROI seed. In *GingerALE*, an activation likelihood estimation (ALE) score is calculated at every voxel in the brain (Turkeltaub et al., 2002; Laird et al., 2005; Eickhoff et al., 2009; Turkeltaub et al., 2012; Eickhoff et al., 2012). These ALE scores were then transformed to *p*-values to identify voxels with significantly higher values than that expected under a null distribution. We thresholded each ALE map at a false discovery rate (FDR) threshold of $P < 0.05$, and a minimum cluster size of 250 mm$^3$. A
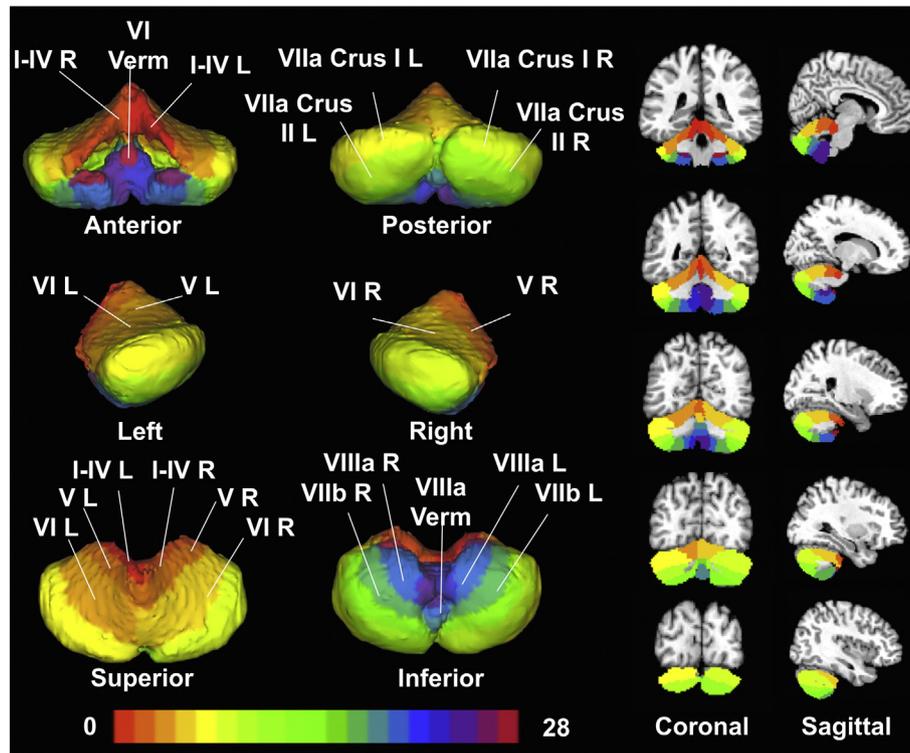
**Fig. 1.** Cerebellar regions of interest. Twenty-eight cerebellar ROIs were generated by thresholding a probabilistic atlas (Diedrichsen et al. (2009)) for each structure at 0.25, indicating that each ROI was consistent across at least 25% of the subjects' anatomical scans. ROIs are shown as volumes (left images) and slices (right images: coronal, top row and sagittal, bottom row).

**Q1 Table 1**

Cerebellar activations archived in BrainMap. Of the 28 cerebellar ROIs considered, 16 were represented by sufficient data for meta-analysis. The volume of each structure is provided in mm³ and is also expressed as a percentage of the total cerebellar volume (average of 114.09 cm³). Also listed is the number of experiments reporting activation coordinates within each ROI, the total number of whole-brain co-activation foci associated with each ROI, and the number of foci reported in each cerebellar ROI.

| Structure | Hemisphere | Volume (mm3) | Volume (%) | Experiments | Co-activations | Metadata foci |
|---|---|---|---|---|---|---|
| *Included structures* | | | | | | |
| I–IV | Left | 3228.7 | 2.83 | 65 | 1055 | 68 |
| | Right | 3548.2 | 3.11 | 66 | 902 | 68 |
| V | Left | 3822 | 3.35 | 114 | 2074 | 122 |
| | Right | 3822 | 3.35 | 166 | 2719 | 173 |
| VI | Left | 8522.5 | 7.47 | 566 | 10,121 | 596 |
| | Right | 7906.4 | 6.93 | 643 | 10,816 | 679 |
| | Vermis | 1905.3 | 1.67 | 117 | 1990 | 126 |
| VIIa Crus I | Left | 12,800.9 | 11.2 | 372 | 6729 | 390 |
| | Right | 12,721 | 11.15 | 370 | 6343 | 383 |
| VIIa Crus II | Left | 9788.9 | 8.58 | 72 | 1501 | 72 |
| | Right | 9252.7 | 8.11 | 63 | 1027 | 65 |
| VIIb | Left | 4586.4 | 4.02 | 28 | 594 | 29 |
| | Right | 4540.8 | 3.98 | 36 | 710 | 37 |
| VIIIa | Left | 4483.7 | 3.93 | 31 | 708 | 31 |
| | Right | 4460.9 | 3.91 | 30 | 658 | 34 |
| | Vermis | 1049.6 | 0.92 | 55 | 941 | 61 |
| Total | | 96,440.3 | 84.51% | 2794 | 48,888 | 2934 |
| | | | | | | |
| *Excluded Structures* | | | | | | |
| VIIa Crus I | Left | 57.1 | 0.05 | 0 | 0 | 0 |
| VIIa Crus II | Left | 433.5 | 0.38 | 11 | 224 | 11 |
| VIIb | Left | 239.6 | 0.21 | 18 | 236 | 18 |
| VIIIb | Left | 3787.8 | 3.32 | 17 | 247 | 17 |
| | Right | 3742.2 | 3.28 | 28 | 390 | 28 |
| | Vermis | 593.3 | 0.52 | 4 | 103 | 5 |
| IX | Left | 3251.6 | 2.85 | 13 | 322 | 13 |
| | Right | 3388.5 | 2.97 | 27 | 425 | 27 |
| | Vermis | 730.2 | 0.64 | 27 | 557 | 27 |
| X | Left | 559 | 0.49 | 2 | 18 | 2 |
| | Right | 593.3 | 0.52 | 5 | 172 | 6 |
| | Vermis | 285.2 | 0.25 | 0 | 0 | 0 |
| Total | | 17,661.1 | 15.48% | 152 | 2694 | 154 |

MACM co-activation map was created for each of the 27 cerebellar ROIs included in this analysis (Fig. 2A, Step 1).

*MACM correlation matrix and hierarchical clustering*

To characterize cerebellar functional organization, we grouped ROIs exhibiting similar whole-brain co-activation profiles using hierarchical clustering analysis (Eickhoff et al., 2010; Bzdok et al., 2012; Liu et al., 2012; Caspers et al., 2013) (Fig. 2A, Step 2). First, a correlation matrix was used to represent the co-activation profile of each of the cerebellar MACMs. This involved loading the thresholded MACM for each ROI into MATLAB (MATLAB 8.3, The MathWorks, Inc., Natick, MA, USA) and creating an $n \times p$ matrix where $n$ is the number of MACMs and $p$ is the number of voxels in the brain. Subsequently, correlation coefficients (Pearson's) between each pair of MACMs were computed to generate an $n \times n$ correlation matrix. Hierarchical clustering was then performed on this $n \times n$ correlation matrix to group cerebellar ROIs with similar co-activation profiles (Fig. 2A, Step 3). The "distance" between each row/column is a measure of the dissimilarity between each row/column, and is defined as 1 minus the respective correlation coefficient (smaller values equal more highly correlated variables). The cophenetic distance, which is the inter-cluster distance between two clusters, can be calculated using a variety of methods (e.g., *single*, *complete*, and *average*). These different methods operate on the distances between observed variables, using the shortest distance, furthest distance, or average distance (unweighted), respectively, to generate clusters. Here, we employed the complete linkage method, which maximizes the distance between clusters to group cerebellar ROIs. The resulting similarities and differences between ROIs were then visualized in a dendrogram in the

MATLAB environment. We then employed a step-wise incremental evaluation starting from the simplistic two-cluster solution to determine an optimal final clustering solution. After assessing the different clustering solutions resulting from the dendrogram, four clusters of cerebellar ROIs were selected for subsequent analysis. In addition, a 7-cluster solution is presented in the Supplementary Material (SF1) to parallel a previously suggested cerebellar parcellation (Buckner et al., 2011).

*Comparison of co-activation profiles*

To characterize the co-activation profile of each cerebellar cluster identified using the above procedures, we created contrast images using *GingerALE*. In these contrast analyses, the whole-brain coordinates extracted from experiments reporting activations for those structures contributing to a single cluster were pooled, and a whole-brain co-activation profile was generated for that specific cluster (e.g., Cluster 1). Additionally, a whole-brain MACM map was generated using the pooled coordinates extracted from experiments reporting activations in structures contributing to all other clusters (e.g., Cluster 2, 3, and 4). In the difference analysis, the experiments contributing to all clusters were pooled, then randomly divided into two groups, with the number of experiments of the first assembly (or pseudo-cluster) equal to that of the original cluster (Cluster 1) and the number of experiments in the second assembly equal to the sum of experiments in all other clusters. ALE statistics were then calculated for each assembly, as well as the difference in ALE statistics. We repeated this process 10,000 times to produce a null distribution of ALE difference-statistics that were then compared to the observed difference-statistics between one cluster's
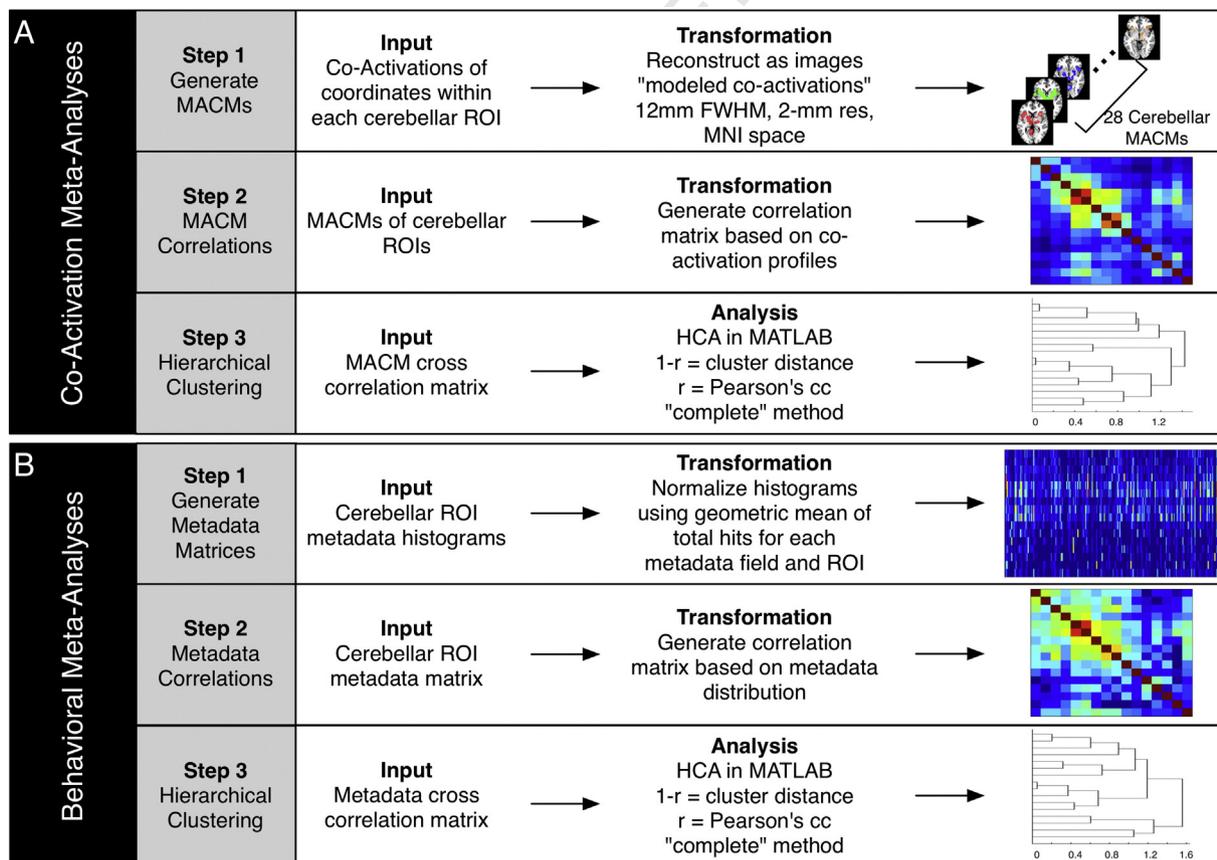


**Fig. 2.** Meta-analysis processing pipelines. (A) Data processing for the *co-activation* meta-analyses was carried out in three steps: Step 1: Coordinates of activation falling within each cerebellar ROI and all corresponding co-activation coordinates were downloaded from BrainMap, and an ALE-based co-activation map was generated for each ROI. Step 2: A correlation matrix was generated based on the co-activation profiles for each of the cerebellar MACMs. Step 3: Hierarchical clustering was carried out to determine groupings of ROIs with similar co-activation patterns. (B) Data processing for the *behavioral* meta-analyses was similarly carried out in three steps: Step 1: Behavioral metadata histograms were generated based on the number of coordinates reported within each ROI for each behavioral domain, paradigm class, or stimulus type. Step 2: A correlation matrix was created based on the behavioral histograms profiles for each region. Step 3: Hierarchical clustering was carried out to determine groupings of ROIs with similar behavioral profiles.

MACM and the MACM of all other clusters (Eickhoff et al., 2011). We employed a FDR corrected threshold of $P < 0.05$, with minimum cluster volume of 250 mm$^3$ to identify differences in co-activation profiles associated with each cerebellar cluster. This process was repeated for each cluster to examine the cortical locations significantly co-activated with each collection of cerebellar structures.

### Behavioral meta-analyses

#### Cerebellar behavioral metadata histograms

The BrainMap database provides not only the ability to examine the meta-analytic co-activation of a given ROI via its co-activation patterns, but also a region's function using the associated behavioral metadata. In an independent but parallel analysis, we investigated the behavioral properties for each of the cerebellar ROIs using metadata archived in the BrainMap database. According to the BrainMap taxonomy (www.brainmap.org/scribe), there are currently 51 different behavioral domains that describe the cognitive processes isolated by the experimental contrast in a functional neuroimaging study, 96 paradigm classes that describe the task performed, and 46 categories of experimental stimuli that are presented to participants. To assess the functional properties of each ROI, the number of activation foci located within a cerebellar structure for a given behavioral domain, paradigm class, or stimulus type was recorded. Characterizing the cerebellar ROIs according to a single metadata field (i.e. behavioral domain, paradigm class, or stimulus type) could minimize the overall power of grouping structures according to their full metadata distribution. For this reason, the simultaneous use of all three metadata fields gives a unique description of each structure, and provides a more robust solution for similar clustering. An $n \times m$ matrix, $F_{n,m}$, was created where $n$ is the number of ROIs, and $m$ is the total number of metadata annotations (i.e., behavioral domains, paradigm classes, and stimulus types). Due to the broad range of experiments reporting foci in each ROI and the broad range of experiments per metadata field, we employed a methodology to account for differential representations across regions as well as metadata fields. Thus, the geometric mean (Eq. (1)) was used as a normalization method to account for these scaling differences when comparing different ROI metadata distributions (Fig. 2B, Step 1):

$$g_{n,m} = \sqrt{(\#foci)_n (\#metadata)_m}. \tag{1}$$

An $n \times m$ geometric mean matrix was calculated for each ROI and each metadata class, where $(\# foci)_n$ represents the number of foci reported in all behavioral domains, paradigm classes, or stimulus types for the $n$th ROI, and $(\# metadata)_m$ represents the number of foci reported for the $m$th metadata field across the whole cerebellum. An element-by-element division was performed (Eq. (2)) between the metadata frequency matrix and the geometric mean matrix to create the normalized metadata matrix, $T_{n,m}$.

$$T_{n,m} = \frac{F_{n,m}}{g_{n,m}}. \tag{2}$$

Essentially, this step finds the geometric mean of two normalized matrices, one matrix normalized to each ROI's metadata distribution sum, and one matrix normalized to each metadata field's sum across all ROIs. In this way, we were able to simultaneously control for a priori probabilities of identifying an activation in a given region AND that a particular metadata field resulted in an activation.

#### Behavioral correlation matrix and hierarchical clustering

After modeling the functional properties of cerebellar ROIs via BrainMap metadata distributions, we sought to identify which regions exhibited similar behavioral metadata profiles. In a manner similar to that used in the analysis of cerebellar MACMs, an $n \times n$ correlation matrix was created based on each structure's geometric mean normalized metadata histogram (Fig. 2B, Step 2). Hierarchical clustering was performed on the correlation matrix to identify groupings of structures with similar behavioral profiles. Again, the Pearson's correlation distance was used to measure the similarity between different rows/columns, and the *complete* linkage method was used to maximize the distance between clusters (Fig. 2B, Step 3).

#### Comparison of behavioral profiles

Experiments reporting activations within a given region in the brain can be analyzed using BrainMap to determine if the frequency of behaviors associated with those experiments occurs at a rate that is significantly greater than chance. We performed a behavioral domain analysis on each cluster by summing the number of coordinates for each behavioral domain in the ROIs contributing to each cluster. There are five primary behavioral domains in the BrainMap taxonomy: action, cognition, emotion, interoception, and perception. A Chi-squared test was used to determine if the behavioral domain histogram for each cluster differed significantly from that of the entire BrainMap database. In this way, we determined if a robust organization of cognitive function exists within the cerebellum. To further interrogate functional specialization, we performed forward inference analyses to identify the above-chance likelihood of activation in a specific cluster given neurological recruitment of a behavioral sub-domain or paradigm class. Essentially, using a binomial test ($P < 0.05$), we determined if the probability of activation of a specific cluster given a task was significantly higher than the base-rate probability of activating the cluster. Additionally, reverse inference analyses were performed on each cluster to determine the behavioral sub-domains or paradigm classes that were over-represented within each cluster compared to the metadata representation in the BrainMap database. Here, a Chi-squared test ($P < 0.05$) was employed to assess whether the probability of the task given an activation of a cluster was significant (Poldrack, 2006; Nickl-Jockschat **Q20** et al., 2013).

## Results

BrainMap searches revealed that certain cerebellar structures contained very few reported coordinates from task-based experiments. For example, one structure (X Vermis) was found to have zero experiments reporting a coordinate of activation within the volume. As a result, ROIs with less than 30 experiments reporting activations were eliminated from further analysis. We chose 30 experiments as a minimum threshold for representative data inputs because it is consistent with simulation data suggesting that $n$'s approaching 30 are required to meet acceptable standards of reliability in typical fMRI studies (Thirion et al., 2007). Based on this exclusion criterion, 16 of 27 cerebellar ROIs were considered suitable for further analysis. The number of experiments contributing to each ROI is shown in Table 1, along with the corresponding percentage of total cerebellar volume. Although excluding 16 of 28 structures suggests that a significant portion of the cerebellum was omitted from our analysis, the discarded regions were primarily located in the vermis and represented only 15% of total cerebellar volume.

### Co-activation meta-analyses

#### MACM of cerebellar ROIs

First, we generated task-independent MACMs for each cerebellar ROI using the 16 structures that met the minimum requirements for analysis. Each MACM was individually viewed to evaluate whether gross qualitative similarities or differences existed among co-activation profiles (Fig. 3). Not surprisingly, those structures reporting a greater number of experiments with activations yielded more robust co-activation patterns, whereas those structures with a limited number of contributing experiments exhibited less robust patterns. Interestingly,
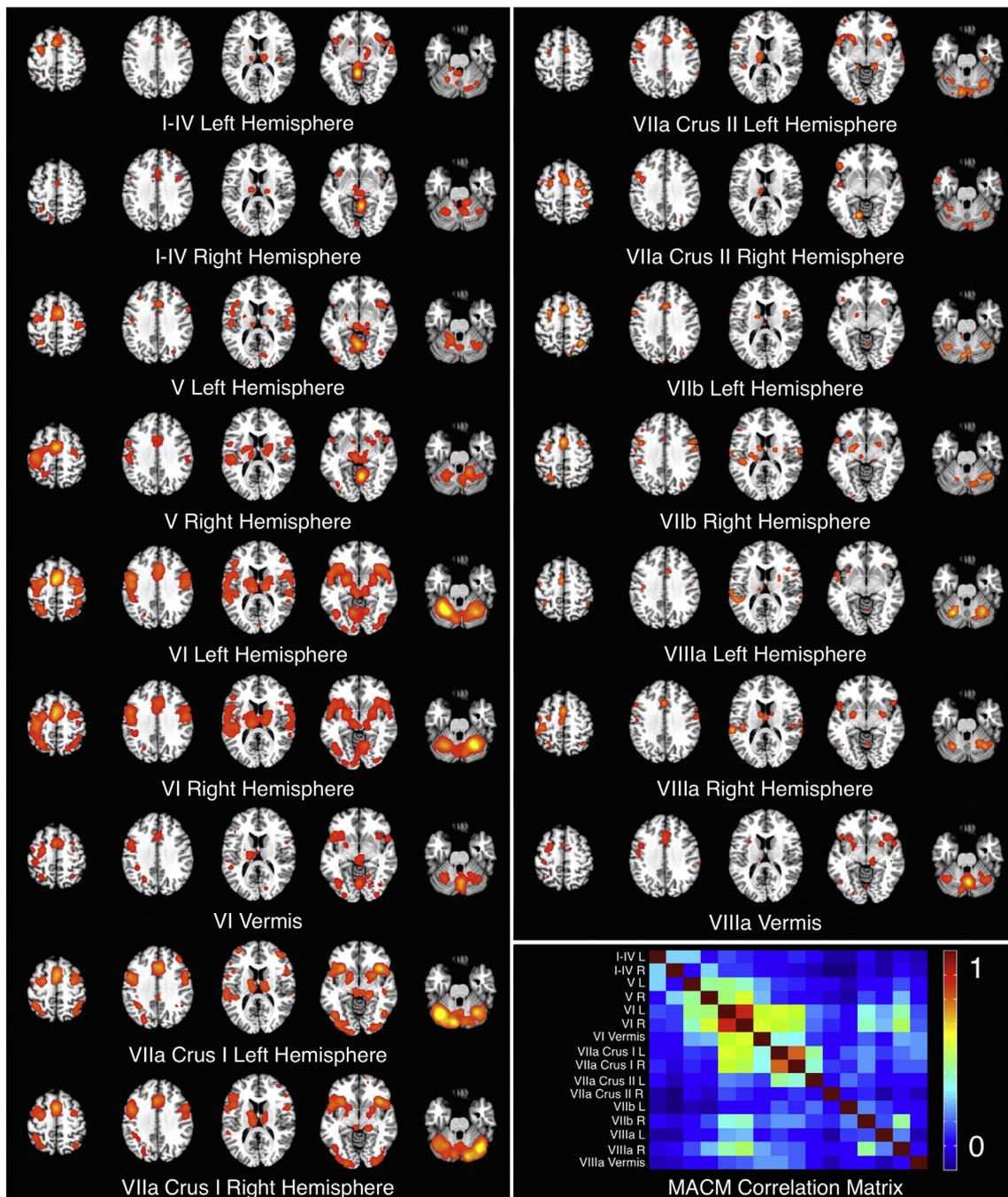
**Fig. 3.** Cerebellar meta-analytic connectivity models (MACMs). The MACMs for each cerebellar ROI were thresholded at *P* < 0.05, FDR-corrected. Inset, bottom right: a diagonal correlation matrix illustrates pairwise correlation coefficients between MACM maps.

most cerebellar structures did not show preference toward unilateral cortical activations. Bilateral co-activations were seen in the frontal, parietal, and temporal lobes for lateralized cerebellar structures.

To identify common regions of co-activation across cerebellar ROIs, we binarized and summed the thresholded probability images (Fig. 4). Regions most consistently observed to co-activate with cerebellar structures included the bilateral thalamus, pre-supplementary motor area (pre-SMA), SMA, and cingulate motor area (CMA), which were included in 14 of the possible 16 cerebellar MACMs. The bilateral insula and lentiform nucleus (putamen) showed consistent activation in 12 MACMs. Regions which were observed to exhibit less consistent co-activation across all MACMs included the motor cortex, bilateral parietal lobules, and frontal gyri (convergence with 8 MACMs), and the temporal gyri and visual and associated visual cortices (convergence

with 4 MACMs). Regions exhibiting the least amount of convergence (i.e., significant co-activation with only one structure) included precuneus, bilateral inferior temporal gyri, and bilateral medial frontal gyri.

*Hierarchical clustering of co-activation patterns*

We next grouped the 16 cerebellar ROIs assessed according to similar co-activation by applying hierarchical clustering to the $n \times n$ correlation matrix using the "correlation" distance metric, and "complete" linkage method. The cophenetic correlation coefficient, which is a quantitative measure of how well the cophenetic distances between variables in the dendrogram correlate with the actual distances between observations, was determined to be 0.7028 for the corresponding dendrogram (Fig. 5A). This can be interpreted in the same way as the
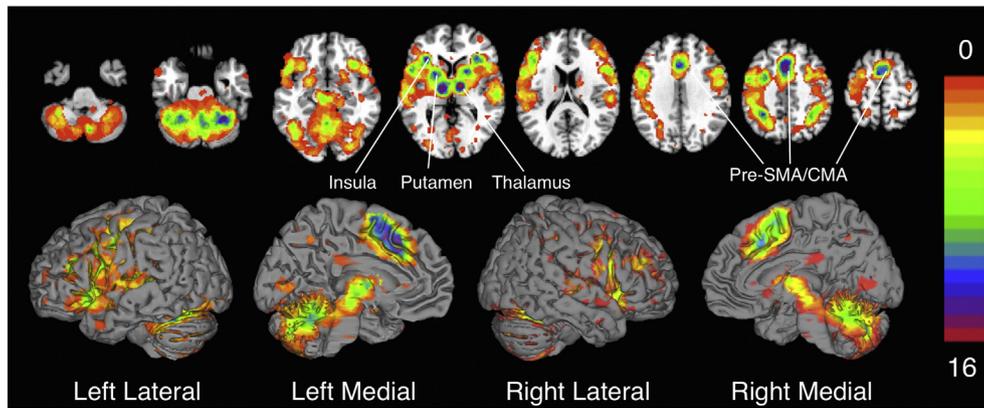
**Fig. 4.** Convergence of MACM results across ROIs. The 16 binarized MACMs were summed into a single image. Areas of convergence across the majority (i.e., at least 12 ROIs) of MACMs included the pre-supplementary motor area (SMA), SMA, cingulate motor area (CMA), bilateral thalamus, putamen, and insula. In contrast, regions of the occipital and parietal lobes showed co-activation with only 1 or 2 cerebellar ROIs.

Pearson's correlation coefficient. The horizontal axis of a dendrogram indicates the dissimilarity between specific groupings of the variables (ROIs in this case) on the vertical axis. For instance, if the union between two ROIs is farther along the horizontal, then the dissimilarity between the two is greater. We identified four well-delineated clusters of ROIs based on the optimal clustering solution using a step-wise incremental
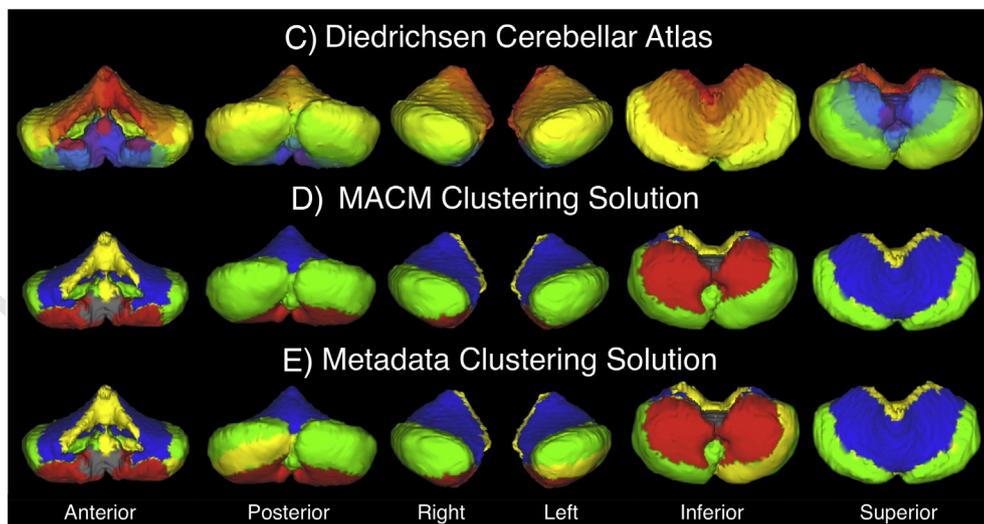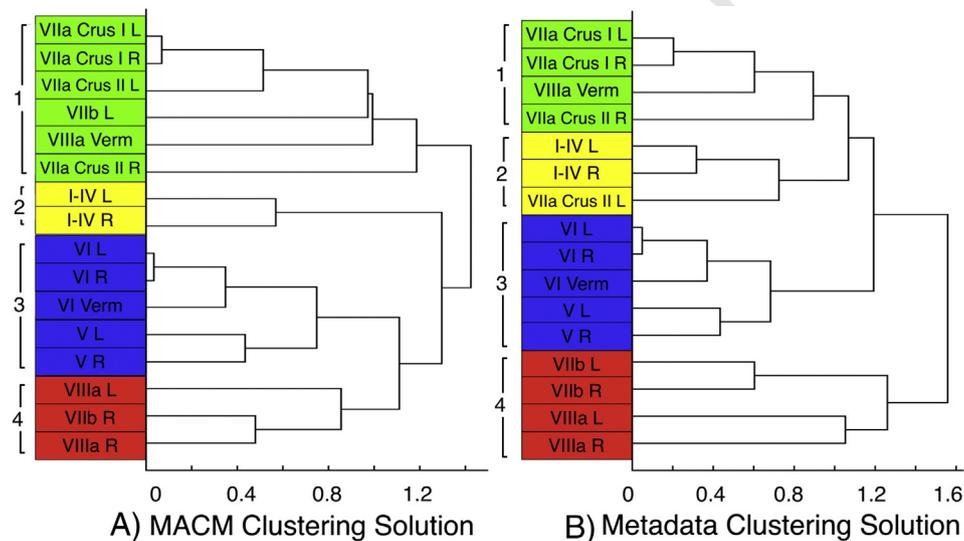


**Fig. 5.** Clustering results for the co-activation and behavioral meta-analyses. (*Top*) The dendrograms illustrate the results of the hierarchical clustering analyses of the correlation matrices calculated from the (A) thresholded MACMs and (B) normalized metadata histograms of each cerebellar ROI. Four well-delineated clusters were identified in each dendrogram, with the clusters in the metadata clustering solution showing 67%, 100%, 100%, and 100%, correspondence with the clusters identified in the MACM clustering solution. (*Bottom*) The Diedrichsen cerebellar ROIs (C) are shown to visually distinguish which structures contributed to the clustering solutions produced from the hierarchical clustering analyses of the (D) MACM co-activation profiles and the (E) behavioral metadata histograms. Structures that were omitted from the co-activation and metadata analyses are displayed in grayscale.

evaluation of the dendrogram. Co-Activation Cluster 1 (Fig. 5A, green) consisted of lobules VIIa Crus I and VIIa Crus II of the left and right hemispheres, VIIb of the left hemisphere and the VIIIa vermis; Co-Activation Cluster 2 (yellow) consisted of lobules I–IV of the left and right hemispheres; Co-Activation Cluster 3 (blue) consisted of lobules V of the left and right hemispheres, lobules VI of the left and right hemispheres, and the VI vermis; and Co-Activation Cluster 4 (red) consisted of lobule VIIb of the right hemisphere, and lobules VIIIa of the left and right hemispheres. This solution was deemed optimal in that clusters were not composed of unilateral structures. Visual inspection of the Diedrichsen atlas and clustering solution (Figs. 5C&D) provides conceptualization of the manner in which cerebellar structures cluster together. The structures omitted from this analysis constituted only a small proportion of cerebellar volume (~15%), and are displayed in grayscale (Figs. 5D&E), whereas the structures analyzed are color-coded in the dendrograms and layouts, according to their respective cluster assignments. For example, the clusters of structures were generally divided into anterior/posterior and superior/inferior groupings: Co-Activation Cluster 1 (Figs. 5A&D, green) was found to include regions that extended across the posterior and middle cerebellum, while, Co-Activation Cluster 2 (yellow) was located in the anterior and far superior cerebellum. Co-Activation Cluster 3 (blue) was located in the superior and mainly anterior cerebellum, while Co-Activation Cluster 4 (red) was observed in the inferior mainly anterior cerebellum. Overall, the clustering results indicated a structured organization to the meta-analytic co-activation of the cerebellum.

### Comparison of co-activation profiles

While many of the cerebellar co-activation profiles appeared similar, subtle differences exist. Fig. 6 illustrates differential cortical projections associated with each cluster compared to an ensemble of all other clusters. Due to the large number of experiments contributing to Co-Activation Clusters 1 and 4, these maps appear more robust than the maps for Co-Activation Clusters 2 and 3. Nonetheless, significant differences emerged, illustrating the differential cortical co-activation of cerebellar clusters. The structures contributing to Co-Activation Cluster 1 (Fig. 6, green), located in the posterior and middle portion of the cerebellum, exhibited distinct co-activation with the bilateral inferior parietal lobes, and inferior frontal gyri. We note that a similar co-activation topography with this cluster has been previously described (Balsters et al., 2014). Co-Activation Cluster 2 (Fig. 6, yellow), in the anterior and far superior cerebellum, showed distinct co-activation with the brainstem, the left ventral lateral and right lateral dorsal nuclei of the thalamus, and to a lesser extent, the bilateral insula. Co-Activation Cluster 3 (Fig. 6, blue), in the superior and anterior cerebellum, exhibited distinct co-activation with the left precentral and postcentral gyri and middle portions of the cingulate cortex. Again, this co-activation profile was demonstrated by the work performed by Balsters et al. (2014). Lastly, Co-Activation Cluster 4 (Fig. 6, red), in the anterior and inferior cerebellum, differentially co-activated with the bilateral precentral gyri, cingulate gyrus, bilateral insula, and bilateral superior temporal gyri.

### Behavioral meta-analyses

#### Metadata histograms of cerebellar structures

In the previous section, we established that separate groupings of cerebellar ROIs showed distinct whole-brain co-activation patterns. Using the metadata catalogued in BrainMap, we aimed to likewise determine if cerebellar ROIs showed distinct behavioral profiles. The resulting histograms were representative of the percentage of activation occurrence for each behavioral domain, paradigm class, or stimulus type (Fig. 7). Visual inspection of the normalized metadata histograms revealed heterogeneous distributions across structures and metadata class. Histograms for those ROIs reporting fewer coordinates (e.g., lobules VII and VIIIa) appear sparsely distributed because certain behavioral domains or paradigms are not represented within that structure. Most other regions appear to be well represented across all behavioral domains and paradigms, with prominent peaks evident in a few structures. The behavioral domains most represented across structures included action (execution), cognition (language), and emotion. This could largely be due to the fact that these three behavioral domains are highly represented in the BrainMap database. Nonetheless, the observation that these behavioral domains appear frequently further illustrates the functional diversity of the cerebellum. The paradigm classes most represented across all cerebellar structures were finger tapping, reading, pain monitor/discrimination, and reward tasks.

#### Hierarchical clustering of behavioral histograms

Similar to the co-activation meta-analysis, hierarchical clustering analysis was applied to the $n \times n$ correlation matrix of the behavioral histograms using the "correlation" distance metric, and "complete" linkage method. The resulting dendrogram (Fig. 5B) yielded a corresponding cophenetic correlation coefficient of 0.7611. Once again, four
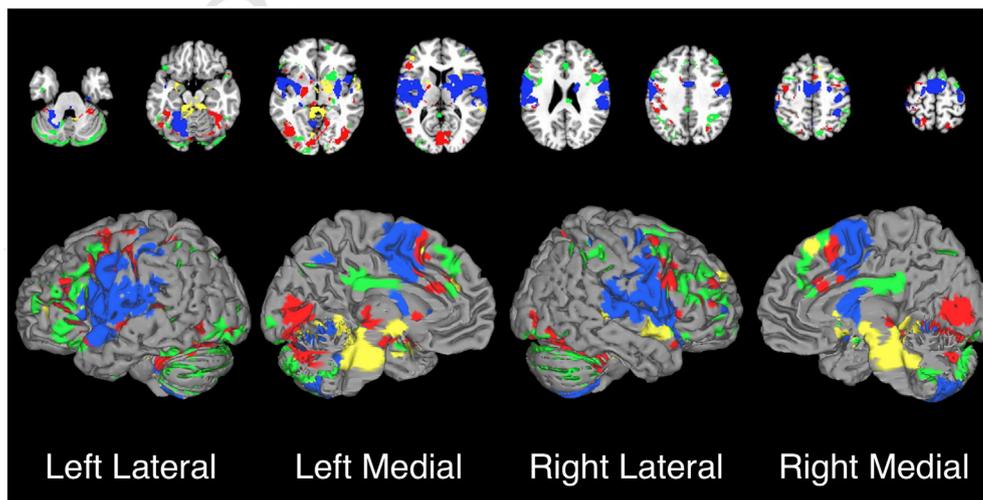


**Fig. 6.** Difference maps from cluster contrast studies. *GingerALE* was used to determine differences between each cluster's whole-brain co-activation profile and the co-activation profile from all other clusters. These maps represent areas of greater co-activation with a particular cluster in comparison to all other cerebellar clusters. The color of each map reflects its corresponding cluster and match the color scheme in Fig. 5D: green = Cluster 1; yellow = Cluster 2; blue = Cluster 3; red = Cluster 4. Each of the 4 ALE-based differential co-activation maps was thresholded at $P < 0.05$, FDR-corrected.
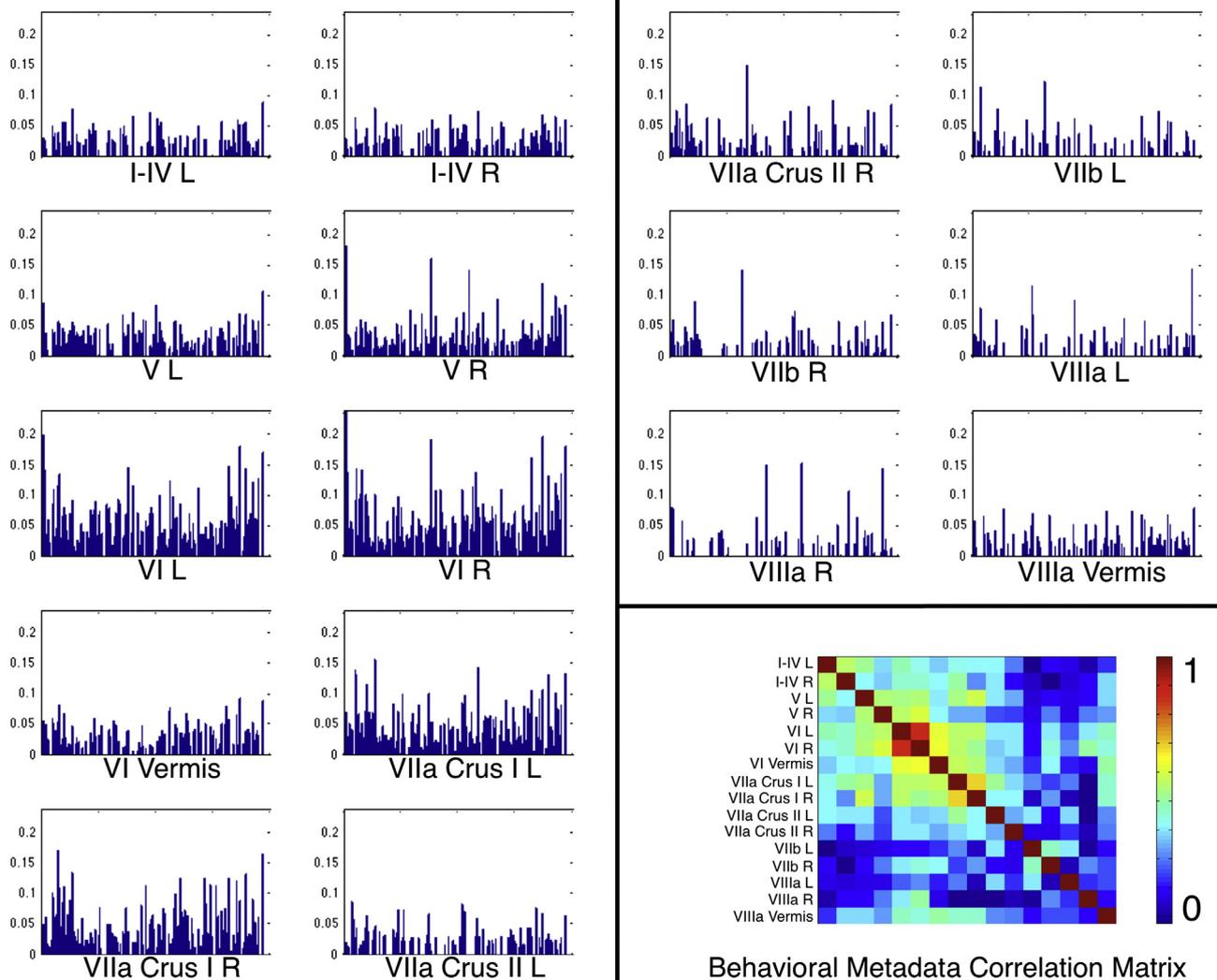
**Fig. 7.** Cerebellar ROI metadata histograms. Behavioral metadata distributions normalized using the geometric mean for each BrainMap class and each cerebellar ROI are shown to enable visual assessment of differences between behavioral profiles. The normalized values are shown here to eliminate any bias toward total experiment number for a single structure and total foci reported for each metadata class. Inset, bottom right: a diagonal correlation matrix illustrates pairwise correlation coefficients between behavioral histograms.

well-delineated clusters were identified through a step-wise incremental evaluation of the dendrogram. Behavioral Cluster 1 (Fig. 5B, green) consisted of lobules VIIa Crus I of the left and right hemispheres, VIIa Crus II of the right hemisphere, and the VIIIa vermis; Behavioral Cluster 2 (yellow) consisted of lobules I–IV of the left and right hemispheres, and VIIa Crus II of the left hemisphere; Behavioral Cluster 3 (blue) consisted of lobules V and VI of the left and right hemispheres, and the VI vermis; and Behavioral Cluster 4 (red) consisted of lobules VIIb and VIIIa of the left and right hemispheres. Similar to the MACM clustering results, clusters consisted of structures that were organized into anterior/posterior and superior/inferior groupings: Behavioral Cluster 1 (Figs. 5 B&E, green) was located in posterior and middle cerebellum; Behavioral Cluster 2 (yellow) primarily in the anterior and far superior cerebellum; Behavioral Cluster 3 (blue) in superior and mainly anterior cerebellum; and Behavioral Cluster 4 (red) in inferior and mainly anterior cerebellum.

Overall, there was a notable degree of similarity between the co-activation based and behavioral-based clustering solutions. Structures in Co-Activation Clusters 2, 3, and 4 are all similarly organized in the Behavioral Clustering solution, while two structures from Co-Activation Cluster 1 were distributed to Behavioral Clusters 2 and 4, respectively. Generally, cerebellar ROIs located spatially near each other were found to exhibit both similar co-activation and behavioral properties.

Therefore, similar results across co-activation and behavioral analyses reinforce the hypothesis that the cerebellum is organized in a way that integrates differential co-activation with behavioral function.

*Comparison of behavioral profiles*

We next examined the significant differences between the behavioral profiles for each cluster and hypothesized that the structures exhibiting similar whole-brain co-activation profiles would also exhibit significant preference toward particular behaviors. Since minor variations between co-activation and behavioral clusters were in fact observed, we performed this comparison analysis on the behavioral properties of the co-activation clusters, for consistency.

Fig. 8 (left) presents four histograms that summarize the main behavioral domain frequencies for Cluster 1 (green), Cluster 2 (yellow), Cluster 3 (blue), and Cluster 4 (red). Domains are represented with a star if the frequencies of cluster activation were found to be significantly over-represented compared to the overall behavioral representation across the BrainMap database via a binomial test (Laird et al., 2010). The results of forward and reverse inference behavioral domain analyses are shown as horizontal bar plots (Fig. 8, middle and right). Results investigating paradigm frequency to determine what types of tasks significantly activate each cluster through forward and reverse inferences analyses are presented in Fig. 9.
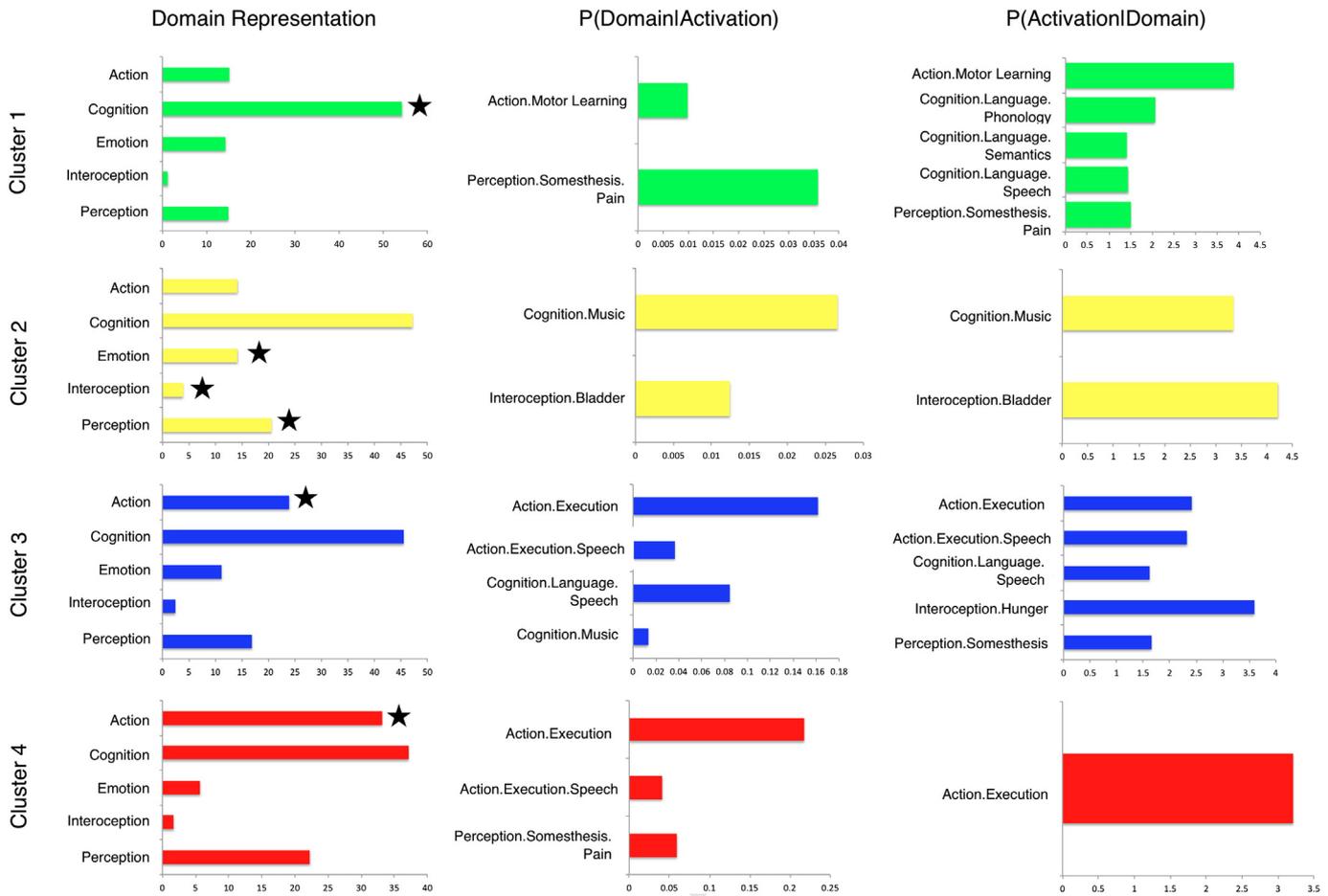
**Fig. 8.** Behavioral domain and sub-domain distributions for cerebellar clusters. The number of domain hits reported for each ROI contributing to the clusters were summed, and expressed in the left column as a percentage of the total number of domain hits within that ROI Those parent domains significantly over-represented with respect to the BrainMap database are indicated with a star. Distributions reflect the BrainMap behavioral distribution, and it is the variation from BrainMap and across clusters that provide valuable behavioral information for each cluster. The middle column represents behavioral sub-domains that are over-represented in each cluster, and the right column represents the behavioral sub-domains that are most likely to produce an activation in each cluster.

Studies comprising Cluster 1 were significantly associated with the domain of "*Cognition*", and showed preference toward "*Phonology*", "*Semantics*", *and* "*Speech*", as well as "*Motor Learning*" and "*Pain*" behavioral sub-domains. In terms of paradigm classes, drawing tasks, n-back tasks, passive listening, and overt word generation most frequently yielded activations within this region. Cluster 2 was significantly associated with "*Emotion*", "*Perception*", and "*Interoception*" domains, specifically, "*Bladder*" and "*Music*". This region of the cerebellum was found to be significantly activated by paradigms associated with episodic recall, flexion/extension, micturition, music comprehension/production, paired associate recall, and visual distractor/attention. The distribution across a range of domains and paradigms is indicative of the relative behavioral diversity of Cluster 2 compared to Cluster 1. In contrast to Clusters 1 and 2, Clusters 3 and 4 were found to be significantly associated with "*Action*". Furthermore, Cluster 3 showed greater preference toward "*Emotion*" and high prevalence of "*Cognition*", and specifically "*Action.Execution*", "*Execution.Speech*", "*Language.Speech*", "*Music*", *Hunger*, and "*Somesthesis*". Cluster 4 had a higher tendency toward "*Cognition*" as a whole, as well as "*Perception*", yet only "*Action.Execution*", "*Execution.Speech*", and "*Somesthesis.Pain*" reached significance in over-representation. The functional specificity of these regions may be interpreted through paradigm class examination, in which Cluster 3 exhibited more frequent associations with drawing, finger tapping, flexion/extension, isometric force, music comprehension/production, naming, reading recitation/repetition, and tactile monitor/discrimination. However, the cognitive and perceptive tendency of Cluster 4 exhibited more frequent associations with finger tapping, go/no-go, isometric force, recitation/repetition tasks, and tactile monitor/discrimination. Clearly, tasks requiring motor execution will likely result in activation within either Cluster 3 or 4; however, specific mental processes associated with the task being performed dictate which region of the cerebellum will be recruited during task execution.

## Discussion

We independently examined cerebellar organization according to co-activation and behavioral properties in an effort to develop a more complete characterization of the relationship between co-activation and function. Hierarchical clustering was employed to assess the similarity of each cerebellar structure's whole-brain co-activation profile, and of each cerebellar structure's BrainMap metadata distributions. The results of both clustering analyses yielded four clusters composed of structures with a high-degree of correspondence. An evaluation of cortical projections from cerebellar clusters showed differential cerebral co-activation, suggesting that cerebellar compartments are functionally specialized.

### Differential functional zones of the cerebellum

Functional neuroimaging evidence supports the parcellation of the cerebellum into at least three regions associated with sensorimotor, cognitive, and limbic functions (Schmahmann and Caplan, 2006). Traditional theories of functional localization in the cerebellum contend that anterior and inferiorly located structures are associated with motor and coordination functions (Hoshi and Tanji, 2007; Passingham and Toni,
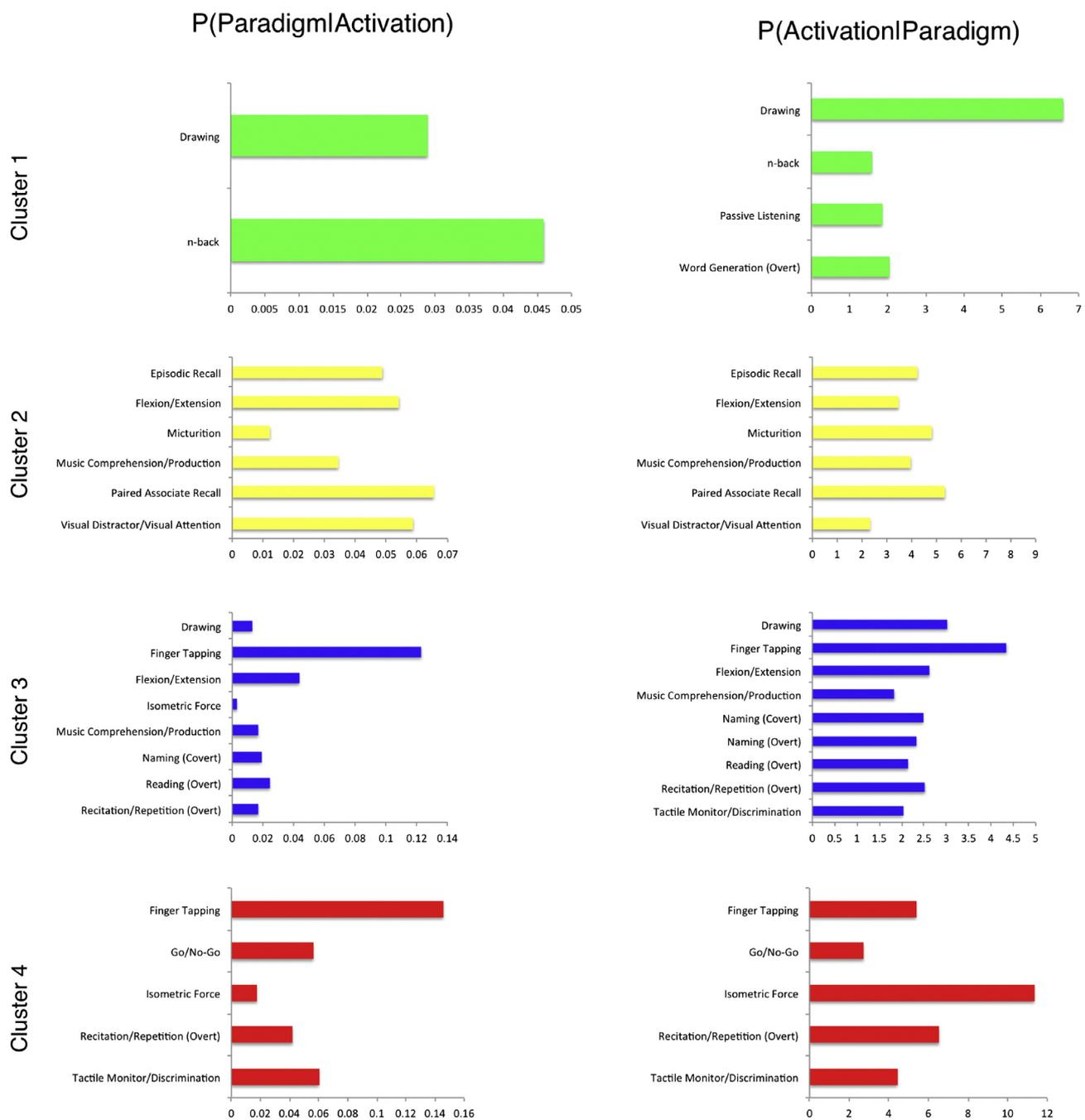
**Fig. 9.** Paradigm class distributions for cerebellar clusters. Experiments in BrainMap are coded according to a taxonomy that describes the type of task subjects performed in the scanner. This information provides further insight into the specific cognitive processes occurring where behavioral domain information alone could lead to vague interpretations. The middle column represents paradigm classes that are over-represented in each cluster, and the right column represents the paradigm classes that are most likely to produce an activation in each cluster.

2001; Rathelot and Strick, 2009), lateral regions are associated with cognitive functions (Imamizu et al., 2003), and that the vermis, fastigial nucleus and flocculondular lobes are involved in affective behavior through structural connectivity with the amygdala and hypothalamus (Hu et al., 2008). In addition, evidence suggests a more complex organization of function such that a medial-to-lateral functional gradient may exist within cerebellar compartments (Makris et al., 2005).

Beyond the central premise of the cerebellum as a motor processing and coordination center, the cerebellum has also been consistently implicated during cognitive processing (Schmahmann and Caplan, 2006). Our findings are consistent with this general notion, but also specify which cortical regions show strong co-activation with the cerebellum. In the present study, Cluster 1 consisted of lobules VIIa Crus I and II of the left and right hemispheres, as well as VIIb of the left hemisphere and the VIIIa vermis. These regions have been purported to be associated with the default mode network (Buckner et al., 2011), demonstrate functional connectivity with prefrontal regions (O'Reilly et al., 2010) and with cerebellar lobules VII, IX, and X (Bernard et al., 2012). Additionally, the structures associated with Cluster 1 showed preferential co-activation with the medial superior frontal gyrus, rostral anterior cingulate cortex, and inferior and middle frontal gyri (Fig. 6, green), which are integral to sustained attention (Bonnelle et al., 2011), working memory (Bennett et al., 2013), and self-control (Aron et al., 2014). Our results correspond well to the designation of Cluster 1 as a zone of high-level cognitive processing, in which the tasks that most likely to be recruited were drawing, n-back, and word generation (Fig. 8). **Q21**

Cluster 2 consisted of the combined lobules I–IV of the left and right cerebellar hemispheres. Dissociation of lobules I–IV tends to be problematic due to the relatively small volume of each cerebellar gyrus, consequently; these lobules are often grouped as a singular structure in the literature. Evidence suggests that lobule IV projects to the primary motor area through the ventrolateral thalamic nuclei (Molinari et al., 2002), as well as the somatosensory cerebral network (Buckner et al., 2011). Resting-state cortico–cerebellar connectivity links lobules I–IV with other cerebral motor regions (Bernard et al., 2012), but also with amygdala and hippocampal regions (Sang et al., 2012). These lobules demonstrated preferential co-activation with the superior temporal gyrus (Fig. 6), which is involved in auditory working memory and previously associated with cerebellar function (Salmi et al., 2009), the perception of emotions in facial stimuli (Bigler et al., 2007; Radua et al., 2009), and is important in the transmission of information between the amygdala and prefrontal cortex (Adolphs, 2003; Bigler et al., 2007) during social cognition. Our results indicated that the tasks that most likely to activate these regions were quite heterogeneous, including flexion/extension, micturition, paired associate recall, and visual attention (Fig. 8). While these results clearly demonstrate Cluster 2's involvement across multiple mental processes, they also align well with the presented evidence that this is a zone of functional heterogeneity.

Cluster 3 consisted of lobules V and VI of the left and right hemispheres and vermis, and is most commonly implicated in studies of motor learning (Debaere et al., 2003), and showed co-activation with the primary motor cortex (Bernard et al., 2012), as well as other anterior cerebellar lobules. Lobule VI represents a transition region between the anterior motor networks and posterior cognitive/associative networks (Bernard et al., 2012), and this was evident in the present study through significant co-activation of sensory and motor cortices, as well as the insula and superior temporal gyrus (Fig. 6). Additionally, Desmond et al. (1997) hypothesized that lobule VI receives afferent information from frontal lobes during articulatory control processes of verbal working memory, and is activated during simple letter repetition tasks. Here, our results indicate that tasks such as finger tapping, flexion/extension, music comprehension, naming, reading, and recitation/repetition were most likely to activate these cerebellar regions, indicating a link to motor processes requiring cognitive input (Fig. 8).

Cluster 4 consisted of lobules VIIb and VIIIa and primarily correlated with the anterior cerebellar lobules (Bernard et al., 2012), which is consistent with motor representation in these lobules (Kelly and Strick, 2003; Stoodley and Schmahmann, 2009; Stoodley et al., 2012). Cluster 4 showed significant co-activation with precuneus (Fig. 6) and inferior parietal lobe (Clower et al., 2001), and Buckner et al. (2011) described these lobules as a secondary motor representation region of the cerebellum. In the present study, tasks such as finger-tapping, isometric force, and tactile monitor/discrimination were observed to consistently activate these regions, suggesting an association with motor processes that require perceptive feedback and strong attentional control (Fig. 8). This is reflected in the report of spatial attention deficits in individuals with cerebellar abnormalities in inferior lobules (VI–VIII; Townsend et al., 2013).

While the functional organization of the cerebellum has been addressed across several previous studies, there are a number of between-study differences in focus and implementation. Importantly, we observed congruence between resting-state functional connectivity profiles derived for cerebellar lobules (Sang et al., 2012), and the meta-analytic co-activation maps derived here. For example, we observed motor cortex co-activation with lobules V and VI of the left and right hemispheres, and prefrontal cortex co-activation with VIIa Crus I and VIIa Crus II of the left and right hemispheres. Buckner et al. (2011) described, on a voxel-wise basis, functional mirroring across the mid-axial plane of the cerebellum through whole-brain intrinsic correlations during the resting state, and subsequently demonstrated that functionally distinct regions of the cerebellum correspond to differential cortical projections. However, their results were driven by forcing cerebellar organization into either 7 or 17 clusters reflecting the cerebral networks established in Yeo et al. (2011). Similarly, Bernard et al. (2012) investigated within-cerebellar connectivity using voxel-wise resting-state functional correlations, and identified 20 cerebellar clusters. While this solution resembled the 17-cluster solution of Buckner et al. (2011), it lacked the inclusion of whole-brain intrinsic correlations in defining cerebellar organization. Bernard and Seidler (2013), shifted from a functional organization of the cerebellum toward a morphological approach, and identified 4 clusters of cerebellar regions based on similar volumetric proportions of cerebellar structures. Despite the methodological differences across these studies, some degree of convergence has emerged that supports an anterior/superior region of the cerebellum exhibiting functional connectivity with motor regions, and a posterior region exhibiting functional connectivity to prefrontal regions.

In contrast to resting state functional connectivity techniques, meta-analysis approaches offer added utility in that they are not limited by the absence of behavioral function. Meta-analyses are advantageous because they can integrate findings across numerous task-based studies to reveal not only significant co-activation, but also functional specificity. In particular, Balsters et al. (2014) aggregated select structures of the cerebellum into two large-scale clusters to investigate whole-brain meta-analytic co-activation based on previous determination of distinctive cerebellar connectivity with prefrontal and motor areas. Whole-brain co-activation of cerebellar lobules V, VI, VIIb, and VIII of the left and right hemispheres was compared to that of the left and right lobules VIIa Crus I and II. The functional organization presented in the current study through clustering methods exhibits similarity to the results of Balsters et al. (2014) which relied on a priori hypotheses about cerebellar functional connectivity. We identified that the cerebellar lobules VIIa Crus I and II grouped together in Cluster 1, demonstrated similar co-activation with the prefrontal regions, while lobules V and VI of Cluster 3 exhibited significant co-activation with motor regions. The current study utilized a data-driven approach (clustering) to organize cerebellar structures based on whole-brain meta-analytic co-activation, as well as behavioral function. Notably, the current results delineated two sub-regions in the single "motor" cluster presented in Balsters et al. (2014). Specifically, cerebellar lobules V and VI (anterior) demonstrate differential connectivity compared to VIIb and VIII (posterior), and serve functionally distinct roles despite a purely "motor" association. Furthermore, the metadata analyses utilized in the current study provide functional distinctions between Clusters 3 and 4 as having preferences toward cognitive and perceptive behaviors, respectively. Thus, the results of the current meta-analysis elaborate on the findings of Balsters et al. (2014) and provide a more refined parcellation of the cerebellum utilizing both co-activation and function.

### Toward a unified functional model of the cerebellum

The integration and coordination of motor and sensory signals has been well established as a fundamental function of the cerebellum. However, increasing evidence supports the involvement of the cerebellum as a vital component of information processing during higher-order cognition, yet the distinctive role the cerebellum plays in these processes continues to be unclear. It has been posited that the cerebellum functions as a forward controller (D'Angelo and Casali, 2013), modulating cerebro–cognitive processing through high frequency (10–40 Hz) activation peaks (Buzsaki, 2006). The cerebellum regulates a series of highly segregated cortico–cerebellar loops, exhibiting indirect connectivity efferently through the deep cerebellar nuclei, and afferently through the anterior pontine nuclei (Gomi and Kawato, 1992; Percheron et al., 1996). The cerebellum is also connected with the basal ganglia, including the dorsal striatum (caudate and putamen), through disynaptic inputs via several thalamic nuclei (Hoshi et al., 2005). Cerebellar co-activation with regions of the pre-SMA, SMA, and cingulate motor areas indicates involvement with the cognitive control and execution of motor actions (Akkal et al., 2007; Nachev et al., 2008; Amiez and

Petrides, 2014), while regions in the anterior cingulate and insular cortices exhibit involvement in error-processing and subsequent behavioral adjustments (e.g., Danielmeier et al., 2011). Furthermore, motor responses are critically associated with dopaminergic function (Durieux et al., 2011; Rogers et al., 2013), as is error-processing (Holroyd and Coles, 2002). Involvement in these motor and cognitive functions is consistent with theories highlighting a role of the cerebellum in regulating dopaminergic function and serving as a forward controller and toggling cortical circuits between automatic and controlled processes (Dosenbach et al., 2006; Ramnani, 2014). Given the diverse range of task-based meta-analytic evidence reported here, it is indeed conceivable that the cerebellum modulates an array of cognitive functions by predicting neurological consequences of a given stimulus, and providing corrective signals in the presence of novelty or errors (Wolpert et al., 1998; Ito, 2008). Bilateral regions of the cerebellum are recruited during the initiation of a variety of cognitive tasks (Dosenbach et al., 2006), requiring differential responses (speech, vision), and this recruitment wanes during sustained activity. More importantly, cerebellar involvement has been observed during error trials (Schlerf et al., 2012; Becerril and Barch, 2013), suggesting that the cerebellum plays an important role in integrating an "anticipatory" neural state with differential cognitive mental responses.

A close examination of the tasks that most consistently activated our observed cerebellar clusters suggests that these tasks require a consistent evaluation and modification of neuronal signals from the cerebral cortex. A recent meta-analysis (Keren-Happuch et al., 2014) demonstrated cerebellar involvement in a range of behaviorally diverse tasks involving temporal attention. Lobules contributing to Cluster 4 are heavily involved in motor tasks, but a clear over-representation in the cognition domain and significant activation with the go/no-go task indicate this region may contribute to generating time-based expectancies of sensory information (Ghajar and Ivry, 2009). Cerebellar involvement in language processing and verbal working memory has been clinically demonstrated through dysfunction in language acquisition and dyslexia (Nicolson et al., 2001), and impairment of working memory (Justus et al., 2005). Furthermore, Ravizza et al. (2005), suggests that the cerebellum is involved in phonological encoding and in strengthening memory traces. Desmond et al. (1997) identified lobules VI and VII as being significant to these mental processes, and not surprisingly, Clusters 1 and 3 were activated by working memory, word generation, recitation/repetition, naming or music comprehension/production tasks. Regions of Cluster 3, although primarily associated with motor tasks, are thought to exist as a transition between the motor anterior cerebellum and cognitive posterior cerebellum as noted above. The premise that the cerebellum contributes to a number of cognitive processes is not novel, and the current study elaborates on models proposing that the cerebellum acts as a forward controller (Miall et al., 1993; Ito, 2005; Ramnani, 2006). Through meta-analytic methods, our results confirm the existence of a functional topography of the cerebellum previously established through both resting-state connectivity-based analyses and meta-analytic methods; and consequently, we identified a number of tasks and mental processes attributed to specific regions of the cerebellum that support the notion that the cerebellum integrates cortical responses with predictive feedback.

*Methodological considerations and limitations*

Twelve of 27 cerebellar ROIs were omitted from this analysis due to a low number of experiments reporting activation within the restrictive confines of those ROIs. These structures are located inferiorly, and as a result, to achieve maximal cerebral coverage, are often excluded during imaging sessions when framing the FOV. In addition, the ROIs we utilized were normalized to a standardized space, which yielded several ROIs of negligible volume (i.e., <1% total cerebellar volume, Table 1, column 4). Thus, we suggest that the omission of these cerebellar regions did not negatively impact the results of our analyses. Ideally, a more comprehensive meta-analysis of the cerebellum would include stronger representation of these regions in the published literature, but given the issues described above, this was not possible.

The clustering approach used in the co-activation analysis was applied to a correlation matrix quantifying the similarity between the *thresholded* MACMs of the 16 ROIs we investigated. To determine the impact of this decision, we additionally performed our analyses using the *unthresholded* MACMs. No substantial differences in cerebellar organization were observed. The *thresholded* MACMs were selected for this analysis to emphasize the co-activation profiles associated with each cerebellar structure, and to describe a functional organization of the cerebellar in this manner.

In the present study, we used standard and commonly applied meta-analytic approaches to generate the MACM images and behavioral histograms. However, our application of hierarchical clustering methods is relatively novel from a meta-analytic perspective. To this end, we evaluated a step-wise incremental clustering solution of the resulting dendrograms corresponding to each meta-analysis to determine the optimal cerebellar organization. Typically, more quantitative techniques utilizing the inconsistency metric may be employed to assist in determining the appropriate clustering solution; however, given the relatively few number of cerebellar structures included in the analyses, we were unable to converge on a solution. To support our approach, we demonstrate that the clustering solutions chosen yielded high cophenetic distances, indicating a large dissimilarity between each clusters associated co-activation pattern or behavioral metadata distribution. Additionally, increasing the number of clusters yields clusters consisting of single structures, thereby reducing the overall dissimilarity between cluster co-activation and function.

When employing clustering analyses to group similar components of a model together, an investigator must determine which method is optimal. In functional neuroimaging studies, the choice commonly lies between hierarchical or k-means clustering. K-means clustering is useful when a priori hypotheses are made concerning the number of known clusters. In contrast, hierarchical clustering does not force the components into a potentially sub-optimal model number. K-means clustering was investigated here as an alternative method to characterize differences between the two analytic approaches. Using mean silhouette value as a quantitative measure for model numbers 1–16 revealed an optimal model number of 7 clusters. Interestingly, this number reflected the optimal number of clusters identified in Buckner et al. (2011). Using the k-means approach, our particular clustering solution consisted of three clusters comprised of only one structure, and one cluster comprised of 5 structures. Our hierarchical approach provided multiple clusters of single ROIs and additionally exhibited dissimilar results between the co-activation and behavioral analyses (Supp. Fig. 1) at the 7-cluster solution. Given the lack of a meaningful functional structure to these solutions, we chose to move forward with hierarchical clustering for this analysis at a more robust parcellation solution of 4 clusters. However, we are currently investigating the utility of k-means clustering for other related meta-analytic applications in the future.

Much of our present results seek to characterize the organizational structure of the cerebellum using functional metadata derived from broad trends reported in the literature. We acknowledge, however, that neuroimaging evidence has indicated that distinct "micro-zones" exist within cerebellar structures, and these "micro-zones" have distinct functional sub-specialties (Buckner et al., 2011; Imamizu et al., 2003; D'Angelo and Casali, 2013). The structural parcellation scheme developed by Diedrichsen et al. (2009) appears robust, as we were able to identify strong correspondences between our results and previously published work. However, a more fine-grained parcellation scheme of each lobule may lead to more informative assessment of micro-zone functional specialization within cerebellar lobules. Future work will involve connectivity-based parcellation (Eickhoff et al., 2011) of all voxels within the cerebellum to yield an organization of the cerebellum not restricted by atlas-defined anatomical boundaries.

The present study used coordinates archived in the BrainMap database and the ALE algorithm to model whole-brain co-activation of cerebellar structures. One limitation of this approach is that the BrainMap coordinates represent activation peaks or center-of-mass coordinates, and thus the overall extent of activation may not be adequately captured. We acknowledge that modeling through the ALE algorithm does not incorporate extent of the published cluster. However, the current implementation of ALE is the culmination of more than 10 years of steady progress in algorithmic development and refinements (Laird et al., 2005; Eickhoff et al., 2009, 2012; Turkeltaub et al., 2012), and has been shown to perform well in comparison to meta-analysis of the full statistical parametric images (Salimi-Khorshidi et al., 2009). Additionally, we acknowledge that the taxonomy of metadata terms recorded with BrainMap activation coordinates may not adequately capture the full extent of the behavioral or mental state that the subjects were experiencing during a particular experiment. However, the BrainMap project places a strong emphasis on developing a robust taxonomy to classify experiments with metadata terms in order to provide a semantic representation of a given study's overall experimental design, with multiple stages of quality control implemented to ensure that tasks and contrasts are accurately classified. Prior studies have addressed the validity of the BrainMap coding scheme (Fox et al., 2005) and its extension into a formal ontology (Laird and Turner, 2012). Moreover, BrainMap annotations are currently being used as a gold standard in developing automated text-mining approaches (Turner et al., 2013). BrainMap metadata have been used in numerous published meta-analyses to provide functional decodings of brain regions or networks in a number of different domains (Laird et al., 2009a, 2009b; Robinson et al., 2009, 2012; Bzdok et al., 2012; Caspers et al., 2013; Clos et al., 2013; Zald et al., 2014). Meta-analytic techniques that pool data across a diverse range of tasks offer a complementary, task-independent perspective in comparison to task-specific fMRI or task-free resting state fMRI. Each method provides insight into functional brain connectivity, and therefore provides an opportunity to contribute to a coherent, comprehensive, and data-driven model. The MACM approach has been shown to illustrate a different aspect of connectivity and hence organization (Jakobs et al., 2012; Clos et al., 2013) in a way that relates more to function and recruitment during task performance than resting state connectivity. In other words, MACM provides complementary insight to rsFC assessments regarding the connectional organization of specify regions, but also provides a methodology to begin considering the behavioral implications of such connections, which is inherently lacking when focusing purely on the resting-state technique. Assessing the behavioral metadata associated with these MACMs has provided a functional interpretation that elaborates on both anatomical and functional connectivity (Bzdok et al., 2012).

## Conclusions

An appreciation of cerebellar function has progressed beyond the conceptualization as a processing center mediating sensory and motor signals, and its contribution to an array of cognitive processes is evident across the neuroimaging literature. As such, several meta-analyses have aggregated this accumulating data in various ways to characterize the functional organization of the cerebellum. Here, we presented a data-driven investigation into the organization of cerebellar structures defined by a probabilistic atlas utilizing both whole-brain co-activation and behavioral properties. Our results suggest a robust parcellation of cerebellar regions into 4 clusters, primarily driven by the differences in pre-frontal and motor co-activation, which is well-demonstrated across the literature. In addition, functional decoding of cerebellar clusters offers the ability to inform theorizing about the cerebellum's involvement in higher-order cognition.

Supplementary data to this article can be found online at http://dx. doi.org/10.1016/j.neuroimage.2015.05.008.

## Uncited references

Balsters et al., 2010
Collins et al., 1994
Diedrichsen, 2006
Fox and Lancaster, 2002
Fox et al., 1994
Fox et al., 1997
Fox et al., 2001
Nickl-Jockschat et al., 2014
Stoodley and Schmahmann, 2010
Talairach and Tournoux, 1988
Xiong et al., 2000

## References

Adolphs, R., 2003. Cognitive neuroscience of human social behaviour. Nat. Rev. Neurosci. 4, 165–178 (March).

Akkal, D., Dum, R.P., Strick, P.L., 2007. Supplementary motor area and presupplementary motor area: targets of basal ganglia and cerebellar output. J. Neurosci. 27 (40), 10659–10673. http://dx.doi.org/10.1523/JNEUROSCI.3134-07.200.

Allen, G., McColl, R., Barnard, H., Ringe, W.K., Fleckenstein, J., Cullum, C.M., 2005. Magnetic resonance imaging of cerebellar–prefrontal and cerebellar–parietal functional connectivity. Neuroimage 28, 39–48 (July 14).

Amiez, C., Petrides, M., 2014. Neuroimaging evidence of the anatomo-functional organization of the human cingulate motor areas. Cereb. Cortex 24 (3), 563–578.

Aron, A.R., Robbins, T.W., Poldrack, R.A., 2014. Inhibition and the right inferior frontal cortex: one decade on. Trends Cogn. Sci. 18 (4), 177–185 (April).

Balsters, J.H., Cussans, E., Diedrichsen, J., Phillips, K.A., Preuss, T.M., Riling, J.K., Ramnani, N., 2010. Evolution of the cerebellar cortex: the selective expansion of prefrontal-projecting cerebellar lobules. Neuroimage 49 (3), 2045–2052.

Balsters, J.H., Laird, A.R., Fox, P.T., Eickhoff, S.B., 2014. Bridging the gap between functional and anatomical features of cortico–cerebellar circuits using meta-analytic connectivity modelling. Hum. Brain Mapp. 35 (7), 3152–3169 (Jul).

Becerril, K.E., Barch, D.M., 2013. Conflict and error processing in an extended cingulo–opercular and cerebellar network in schizophrenia. Neuroimage Clin. 3, 470–480.

Bennett, I.J., Rivera, H.G., Rypma, B., 2013. Isolating age-group differences in working memory load-related neural activity: assessing the contribution of working memory capacity using a partial-trial fMRI method. Neuroimage 72, 20–32 (May 15).

Bernard, J.A., Seidler, R.D., 2013. Relationships between cerebellar volume and sensorimotor and cognitive function in young and older adults. Cerebellum 12, 721–737.

Bernard, J.A., Seidler, R.D., Hassevoort, K.M., Benson, B.L., Welsh, R.C., Wiggins, J.L., Jaeggi, S.M., Buschkuehl, M., Monk, C.S., Jonides, J., Peltier, S.J., 2012. Resting state cortico-cerebellar functional connectivity networks: a comparison of anatomical and self-organizing map approaches. Front. Neuroanat. 6 (31), 1–19 (August 10).

Bigler, E.D., Mortensen, S., Neeley, E.S., Ozonoff, S., Krasny, L., Johnson, M., Lu, J., Provencal, S.L., McMahon, W., Lainhart, J.E., 2007. Superior temporal gyrus, language function, and autism. Dev. Neuropsychol. 31 (2), 217–238.

Bonnelle, V., Leech, R., Kinnunen, K.M., Ham, T.E., Beckmann, C.F., De Boissezon, X., Greenwood, R.J., Sharp, D.J., 2011. Default mode network connectivity predicts sustained attention deficits after traumatic brain injury. J. Neurosci. 31 (38), 13442–13451 (September 21).

Buckner, R.L., Krienen, F.M., Castellanos, A., Diaz, J.C., Yeo, B.T.T., 2011. The organization of the human cerebellum estimated by intrinsic functional connectivity. J. Neurophysiol. 106, 2322–2345 (July 27).

Buzsaki, G., 2006. Rhythms of the Brain. Oxford University Press US, New York, NY.

Bzdok, D., Laird, A.R., Zilles, K., Fox, P.T., Eickhoff, S.B., 2012. An investigation of the structural, connectional, and functional subspecialization in the human amygdala. Hum. Brain Mapp. 34 (12), 3247–3266 (Jul).

Caspers, J., Zilles, K., Amunts, K., Laird, A.R., Fox, P.T., Eickhoff, S.B., 2013. Functional characterization and differential coactivation patterns of two cytoarchitectonic visual areas on the human posterior fusiform gyrus. Hum. Brain Mapp. 35 (6), 2754–2767 (13 Sep).

Chen, R., 2004. Interactions between inhibitory and excitatory circuits in the human motor cortex. Exp. Brain Res. 154, 1–10.

Clos, M., Amunts, K., Laird, A.R., Fox, P.T., Eickhoff, S.B., 2013. Tackling the multifunctional nature of Broca's region meta-analytically: co-activation-based parcellation of area 44. Neuroimage 83, 174–188.

Clower, D.M., West, R.A., Lynch, J.C., Strick, P.L., 2001. The inferior parietal lobule is the target of output from the superior colliculus, hippocampus, and cerebellum. J. Neurosci. 21 (16), 6283–6291 (August 15).

Collins, D.L., Neelin, P., Peters, T.M., Evans, A.E., 1994. Automatic 3D intersubject registration of MR columetric data in standardized Talairach space. J. Comput. Assist. Tomogr. 18, 192–205.

D'Angelo, E., Casali, S., 2013. Seeking a unified framework for cerebellar function and dysfunction: from circuit operations to cognition. Front. Neural Circuits 6 (116), 1–23 (January).

Danielmeier, C., Eichele, T., Forstmann, B.U., Tittgemeyer, M., Ullsperger, M., 2011. Posterior medial frontal cortex activity predicts post-error adaptation in task-related visual and motor areas. J. Neurosci. 31 (5), 1780–1789.

Debaere, F., Wenderoth, N., Sunaert, S., Van Hecke, P., Swinnen, S.P., 2003. Changes in brain activation during the acquisition of a new bimanual coordination task. Neuropsychologia 42, 855–867 (December 10).

Desmond, J.E., Gabrieli, J.D.E., Wagner, A.D., Ginier, B.L., Glover, G.H., 1997. Lobular patterns of cerebellar activation in verbal working-memory and finger-tapping tasks as revealed by functional MRI. J. Neurosci. 17 (24), 9675–9685 (December 15).

Diedrichsen, J., 2006. A spatially unbiased atlas template of the human cerebellum. Neuroimage 33, 127–138.

Diedrichsen, J., Balsters, J.H., Flavell, J., Cussans, E., Ramnani, N., 2009. A probabilistic MR atlas of the human cerebellum. Neuroimage 46, 39–46 (Feb. 5).

Dobromyslin, V.I., Salat, D.H., Fortier, C.B., Leritz, E.C., Beckmann, C.F., Milberg, W.P., McGlinchey, R.E., 2012. Distinct functional networks within the cerebellum and their relation to cortical systems assessed with independent component analysis. Neuroimage 60, 2073–2085 (February 9).

Dosenbach, N.U.F., Visscher, K.M., Palmer, E.D., Miezin, F.M., Wenger, K.K., Kang, H.C., Burgund, E.D., Grimes, A.L., Schlaggar, B.L., Petersen, S.E., 2006. A core system for the implementation of task sets. Neuron 50, 799–812 (June 1).

Durieux, P.F., Schiffmann, S.N., de Kerchove d'Exaerde, A., 2011. Differential regulation of motor control and response to dopaminergic drugs by D1R and D2R neurons in distinct dorsal striatum subregions. Eur. Mol. Biol. Organ. J. 31 (3), 640–653.

Eickhoff, S.B., Laird, A.R., Grefkes, C., Wang, L.E., Zilles, K., Fox, P.T., 2009. Coordinate-based activation likelihood estimation meta-analysis of neuroimaging data: a random-effects approach based on empirical estimates of spatial uncertainty. Hum. Brain Mapp. 30, 2907–2926.

Eickhoff, S.B., Bzdok, D., Laird, A.R., Roski, C., Caspers, S., Zilles, K., Fox, P.T., 2011. Co-activation patterns distinguish cortical modules, their connectivity and functional differentiation. Neuroimage 57, 938–949.

Eickhoff, S.B., Bzdok, D., Laird, A.R., Kurth, F., Fox, P.T., 2012. Activation likelihood estimation revisited. Neuroimage 59, 2349–2361.

Fox, P.T., Lancaster, J.L., 2002. Mapping context and content: the BrainMap model. Nat. Rev. Neurosci. 3, 319–321.

Fox, P.T., Mikiten, S., Davis, G., Lancaster, J.L., 1994. BrainMap: a database of human functional brain mapping. In: Thatcher, R.W., Zeffiro, T., Huerta, M. (Eds.), Advances in Functional Neuroimaging: Technical Foundations. Academic Press, Orlando, pp. 95–106.

Fox, P.T., Lancaster, J.L., Parsons, L.M., Xiong, X.H., Zamarripa, F., 1997. Functional volumes modeling: theory and preliminary assessment. Hum. Brain Mapp. 5, 306–311.

Fox, P.T., Huang, A., Parsons, L.M., Xiong, J.H., Zamarippa, F., Rainey, L., Lancaster, J.L., 2001. Location-probability profiles for the mouth region of human primary motor–sensory cortex: model and validation. Neuroimage 13, 196–209.

Fox, P.T., Laird, A.R., Fox, S.P., Fox, M., Uecker, A.M., Crank, M., Koenig, S.F., Lancaster, J.L., 2005. BrainMap taxonomy of experimental design: description and evaluation. Hum. Brain Mapp. 25, 185–198.

Ghajar, J., Ivry, R.B., 2009. The predictive brain state: asynchrony in disorders of attention? Neuroscientist 15 (3), 232–242 (June).

Gomi, H., Kawato, M., 1992. Adaptive feedback control models of the vestibulocerebellum and spinocerebellum. Biol. Cybern. 68, 105–114 (June 27).

Greco, C.M., Hagerman, R.J., Tassone, F., Chudley, A.E., Del Bigio, M.R., Jacquemont, S., Leehey, M., Hagerman, P.J., 2002. Neuronal intranuclear inclusions in a new cerebellar tremor/ataxia syndrome among fragile X carriers. Brain 1, 1760–1771 (Aug).

Habas, C., Kamdar, N., Nguyen, D., Prater, K., Beckmann, C.F., Menon, V., Greicius, M.D., 2009. Distinct cerebellar contributions to intrinsic connectivity networks. J. Neurosci. 29 (26), 8586–8594 (July 1).

Holroyd, C.B., Coles, M.G.H., 2002. The neural basis of human error processing: reinforcement learning, dopamine, and the error-related negativity. Psychol. Rev. 109 (4), 679–709.

Hoshi, E., Tanji, J., 2007. Distinctions between dorsal and ventral premotor areas: anatomical connectivity and functional properties. Curr. Opin. Neurobiol. 17 (2), 234–242.

Hoshi, E., Tremblay, L., Féger, J., Carras, P.L., Strick, P.L., 2005. The cerebellum communicates with the basal ganglia. Nat. Neurosci. 8 (11), 1491–1493. http://dx.doi.org/10.1038/nn154.

Hu, D., Shen, H., Zhou, Z., 2008. Functional asymmetry in the cerebellum: a brief review. Cerebellum 304–313.

Imamizu, H., Kuroda, T., Miyauchi, S., Yoshioka, T., Kawato, M., 2003. Modular organization of internal models of tools in the human cerebellum. Proc. Natl. Acad. Sci. U. S. A. 100 (9), 5461–5466 (April 29).

Ito, M., 2005. Bases and implications of learning in the cerebellum — adaptive control and internal model mechanisms. Prog. Brain Res. 148, 95–109.

Ito, M., 2008. Control of mental activities by internal models in the cerebellum. Nat. Rev. Neurosci. 9, 304–313 (April).

Justus, T., Ravizza, S.M., Fiez, J.A., Ivry, R.B., 2005. Reduced phonological similarity effects in patients with damage to the cerebellum. Brain Lang. 10, 304–318 (March).

Kelly, R.M., Strick, P.L., 2003. Cerebellar loops with motor cortex and prefrontal cortex of a nonhuman primate. J. Neurosci. 23 (23), 8432–8444 (September 10).

Keren-Happuch, E., Shen-Hsin, A.C., Moon-Ho, R.H., Desmond, J.E., 2014. A meta-analysis of cerebellar contributions to higher cognition from PET and fMRI studies. Hum. Brain Mapp. 35, 593–615.

Krienen, F.M., Buckner, R.L., 2009. Segregated fronto-cerebellar circuits revealed by intrinsic functional connectivity. Cereb. Cortex 19, 2485–2497 (October).

Laird, A.R., Turner, J.A., 2012. The cognitive paradigm ontology: design and application. Neuroinformatics 10 (1), 57–66 (Jan).

Laird, A.R., Lancaster, J.L., Fox, P.T., 2005. BrainMap: the social evolution of a functional neuroimaging database. Neuroinformatics 3, 65–78.

Laird, A.R., Eickhoff, S.B., Kurth, F., Fox, P.M., Uecker, A.M., Turner, J.A., Robinson, J.L., Lancaster, J.L., Fox, P.T., 2009a. ALE meta-analysis workflows via the BrainMap database: progress towards a probabilistic functional brain atlas. Front Neuroinform. 3 (23), 1–11 (July 09).

Laird, A.R., Eickhoff, S.B., Li, K., Robin, D.A., Glahn, D.C., Fox, P.T., 2009b. Investigating the functional heterogeneity of the default mode network using coordinate-based meta-analytic modeling. J. Neurosci. 29 (46), 14496–14505 (November 18).

Laird, A.R., Robinson, J.L., McMillan, K.M., Tordesillas-Gutierrez, D., Moran, S.T., Gonzales, S.M., Ray, K.L., Franklin, C., Glahn, D.C., Fox, P.T., Lancaster, J.L., 2010. Comparison of the disparity between Talairach and MNI coordinates in functional neuroimaging data: validation of the Lancaster transform. Neuroimage 51, 677–683.

Lancaster, J.L., Tordesillas-Gutierrez, D., Martinez, M., Salinas, F., Evans, A., Zilles, K., Mazziotta, J.C., Fox, P.T., 2007. Bias between MNI and Talairach coordinates analyzed using the ICBM-152 brain template. Hum. Brain Mapp. 28, 1194–1205.

Liu, X., Zhu, X., Qiu, P., Chen, W., 2012. A correlation-matrix-based hierarchical clustering method for functional connectivity analysis. J. Neurosci. 211, 94–102.

Makris, N., Schlerf, J.E., Hodge, S.M., Haselgrove, C., Albaugh, M.D., Seidmann, L.J., Rauch, S.L., Harris, G., Biederman, J., Caviness, V.S., Kennedy, D.N., Schmahmann, J.D., 2005. MRI-based surface-assisted parcellation of human cerebellar cortex: an anatomically specified method with estimate of reliability. Neuroimage 25, 1146–1160 (March 11).

Miall, R.C., Weir, D.J., Wolllpert, D.M., Stein, J.F., 1993. Is the cerebellum a smith predictor? J. Mot. Behav. 25, 203–216.

Miall, R.C., Reckess, G.Z., Imamizu, H., 2001. The cerebellum coordinates eye and hand tracking movements. Nat. Neurosci. 4, 638–644.

Middleton, F.A., Strick, P.L., 1994. Anatomical evidence for cerebellar and basal ganglia involvement in higher cognitive function. Science 266 (5184), 458–461 (21 Oct).

Molinari, M., Filippini, V., Leggio, M.B., 2002. Neuronal plasticity of interrelated cerebellar and cortical networks. Neuroscience 111 (4), 863–870 (May 14).

Moulton, E.A., Elman, I., Pendse, G., Schmahmann, J., Becerra, L., Borsook, D., 2011. Aversion-related circuitry in the cerebellum: responses to noxious heat and unpleasant images. J. Neurosci. 31 (10), 3795–3804 (March 9).

Nachev, P., Kennard, C., Husain, M., 2008. Functional role of the supplementary and pre-supplementary motor areas. Nat. Rev. Neurosci. 9 (11), 856–869.

Nickl-Jockschat, T., Rottschy, C., Thommes, J., Schneider, F., Laird, A.R., Fox, P.T., Eickhoff, S.B., 2014. Neural networks related to dysfunctional face processing in autism spectrum disorder. Brain Struct. Funct. (April 28). **Q44**

Nicolson, R.I., Fawcett, A.J., Dean, P., 2001. Developmental dyslexia: the cerebellar deficit hypothesis. Trends Neurosci. 24 (9), 508–511 (September).

O'Reilly, J.X., Beckmann, C.F., Tomassini, V., Ramnani, N., Johansen-Berg, H., 2010. Distinct and overlapping functional zones in the cerebellum defined by resting state functional connectivity. Cereb. Cortex 20, 953–965 (April).

Passingham, R.E., Toni, I., 2001. Contrasting the dorsal and ventral visual systems: guidance of movement versus decision making. Neuroimage 14 (1 Pt 2), S125–S131.

Percheron, G., Francois, C., Talbi, B., Yelnik, J., Fenelon, G., 1996. The primate motor thalamus. Brain Res. Rev. 22 (2), 93–181.

Poldrack, R.A., 2006. Can cognitive processes be inferred from neuroimaging data? Trends Cogn. Sci. 10 (2), 59–63 (February).

Radua, J., Phillips, M.L., Russell, T., Lawrence, N., Marshall, N., Kalidindi, S., El-Hage, W., McDonald, C., Giampietro, V., Brammer, M.J., David, A.S., Surguladze, S.A., 2009. Neural response to specific components of fearful faces in healthy and schizophrenic adults. Neuroimage 49, 939–946.

Ramnani, N., 2006. The primate cortico–cerebellar system: anatomy and function. Nat. Rev. 7, 511–522.

Ramnani, N., 2014. Automatic and controlled processing in the corticocerebellar system. Prog. Brain Res. 210 (Cerebellar Learning).

Rathelot, J.A., Strick, P.L., 2009. Subdivisions of primary motor cortex based on cortico–motoneuronal cells. Proc. Natl. Acad. Sci. U. S. A. 106 (3), 918–923.

Ravizza, S.M., McCormick, C.A., Schlerf, J.E., Justus, T., Ivry, R.B., Fiez, J.A., 2005. Cerebellar damage produces selective deficits in verbal working memory. Brain 129, 306–320 (November 29).

Reetz, K., Dogan, I, Rolfs, A., Binkofski, F., Schulz, J.B., Laird, A.R., Fox, P.T., Eickhoff, S.B., 2012. Investigating function and connectivity of morphometric findings — exemplified on cerebellar atrophy in spinocerebellar ataxia 17 (SCA17). Neuroimage 62 (3), 1354–1366 (Sep).

Robinson, J.L., Laird, A.R., Glahn, D.C., Lovallo, W.R., Fox, P.T., 2009. Metaanalytic connectivity modeling: delineating the functional connectivity of the human amygdala. Hum. Brain Mapp. 31, 173–184 (July 14).

Robinson, J.L., Laird, A.R., Glahn, D.C., Blangero, J., Sanghera, M.K., Pessoa, L., Fox, P.M., Uecker, A., Friehs, G., Young, K.A., Griffin, J.L., Lovallo, W.R., Fox, P.T., 2012. The functional connectivity of the human caudate: an application of meta-analytic connectivity modeling with behavioral filtering. Neuroimage 60, 117–129.

Rogers, T.D., Dickson, P.E., McKimm, E., Heck, D.H., Goldowitz, D., Blaha, C.D., Mittleman, G., 2013. Reorganization of circuits underlying cerebellar modulation of prefrontal cortical dopamine in mouse models of autism spectrum disorder. Cerebellum 12, 547–556.

Rosch, R.E., Ronan, L., Cherkas, L., Gurd, J.M., 2010. Cerebellar asymmetry in a pair of monozygotic handedness — discordant twins. J. Anat. 217 (1), 38–47 (July).

Salimi-Khorshidi, G., Smith, S.M., Keltner, J.R., Wager, T.D., Nichols, T.E., 2009. Meta-analysis of neuroimaging data: a comparison of image-based and coordinate-based pooling of studies. Neuroimage 45, 810–823.

Salmi, J., Pallesen, K.J., Neuvonen, T., Brattico, E., Korvenoja, A., Salonen, O., Carlson, S., 2009. Cognitive and motor loops of the human cerebro-cerebellar system. J. Cogn. Neurosci. 22 (11), 2663–2676.

Sang, L., Qin, W., Liu, Y., Han, W., Zhang, Y., Jiang, T., Yu, C., 2012. Resting-state functional connectivity of the vermal and hemispheric subregions of the cerebellum with both

the cerebral cortical networks and subcortical structures. Neuroimage 61, 1213–1225 (April 14).

Schlerf, J., Ivry, R.B., Diedrichsen, J., 2012. Encoding of sensory prediction errors in the human cerebellum. J. Neurosci. 32 (14), 4913–4922 (April 4).

Schmahmann, J.D., 1991. An emerging concept: the cerebellar contribution to higher function. Arch. Neurol. 48 (11), 1178–1187.

Schmahmann, J.D., 2004. Disorders of the cerebellum: ataxia, dysmetria of thought, and the cerebellar cognitive affective syndrome. J. Neuropsychiatry Clin. Neurosci. 16, 367–378.

Schmahmann, J.D., Caplan, D., 2006. Cognition, emotion and the cerebellum. Brain 129, 288–292.

Schmahmann, J.D., Pandya, D.N., 1989. Anatomical investigation of projections to the basis pontis from posterior parietal association cortices in rhesus monkey. J. Comp. Neurol. 289 (1), 53–73 (1 Nov).

Schmahmann, J.D., Sherman, J.C., 1998. The cerebellar cognitive affective syndrome. Brain 4, 561–579.

Schmahmann, J.D., Doyon, J., Petrides, M., Evans, A.C., Toga, A.W., 2000. MRI Atlas of the Human Cerebellum. Academic Press, San Diego.

Schweighofer, N., Arbib, M.A., Kawato, M., 1998. Role of the cerebellum in reaching movements in humans. I. Distributed inverse dynamics control. Eur. J. Neurosci. 10 (1), 86–94 (Jan).

Stoodley, C.J., 2011. The cerebellum and cognition: evidence from functional imaging studies. Cerebellum 11, 352–365 (March 4).

Stoodley, C.J., Schmahmann, J.D., 2009. Functional topography in the human cerebellum: a meta-analysis of neuroimaging studies. Neuroimage 44, 489–501.

Stoodley, C.J., Schmahmann, J.D., 2010. Evidence for topographic organization in the cerebellum of motor control versus cognitive and affective processing. Cortex 46, 831–844 (January 11).

Stoodley, C.J., Valera, E.M., Schmahmann, J.D., 2011. Functional topography of the cerebellum for motor and cognitive tasks: an fMRI study. Neuroimage 59, 1560–1570 (August 31).

Strata, P., Scelfo, B., Sacchetti, B., 2011. Involvement of cerebellum in emotional behavior. Physiol. Res. 60 (Suppl. 1), S39–S48 (July 19).

Suzuki, M., Asada, Y., Ito, J., Hayashi, K., Inoue, H., Kitano, H., 2003. Activation of cerebellum and basal ganglia on volitional swallowing detected by functional magnetic resonance imaging. Dysphagia 18, 71–77.

Talairach, J., Tournoux, P., 1988. Coplanar Stereotaxic Atlas of the Human Brain. Thieme Medical, New York, NY.

Thirion, B., Pinel, P., Meriaux, S., Roche, A., Dehaene, S., Poline, J., 2007. Analysis of a large fMRI cohort: statistical and methodological issues for group analyses. Neuroimage 35, 105–120 (January 18).

Tiemeier, H., Lenroot, R.K., Greenstein, D.K., Tran, L., Pierson, R., Giedd, J.N., 2010. Cerebellum development during childhood and adolescence: a longitudinal morphometric MRI study. Neuroimage 49 (1), 63–70 (January 1).

Townsend, J.D., Torrisi, S.J., Lieberman, M.D., Sugar, C.A., Bookheimer, S.Y., Alshuler, L.L., 2013. Frontal-amygdala connectivity alterations during emotion downregulation in bipolar I disorder. Biol. Psychiatry 73, 127–135.

Turkeltaub, P.E., Eden, G.F., Jones, K.M., Zeffiro, T.A., 2002. Meta-analysis of the functional neuroanatomy of single word reading: method and validation. Neuroimage 16, 765–780.

Vahdat, S., Darainy, M., Milner, T.E., Ostry, D.J., 2011. Functionally specific changes in resting-state sensorimotor networks following motor learning. J. Neurosci. 31 (47), 16907–16915 (November 23).

Wildenberg, J.C., Tyler, M.E., Danilov, Y.P., Kaczmarek, K.A., Meyerand, M.E., 2011. High-resolution fMRI detects neuromodulation of individual brainstem nuclei by electrical tongue stimulation in balance-impaired individuals. Neuroimage 56 (4), 2129–2137 (June 15).

Wise, R.J.S., Greene, J., Buchel, C., Scott, S.K., 1999. Brain regions involved in articulation. Lancet 353 (9158), 1057–1061 (March 27).

Wolpert, D.M., Miall, R.C., Kawato, M., 1998. Internal models in the cerebellum. Trends Cogn. Sci. 2 (9), 338–347 (September).

Wu, X., Ashe, J., Bushara, K.O., 2011. Role of olivocerebellar system in timing without awareness. Proc. Natl. Acad. Sci. U. S. A. 108 (33), 13818–13822 (August 16).

Xiong, J., Rao, S., Jerabek, P., 2000. Intersubject variability in cortical activations during a complex language task. Neuroimage 12, 326–339.

Yeo, B.T.T., Krienen, F.M., Sepulcre, J., Sabuncu, M.R., Lashkari, L., Hollinshead, M., Roffman, J.L., Smoller, J.W., Zöllei, L., Polimeni, J.R., Fischl, B., Liu, H., Buckner, R.L., 2011. The organization of the human cerebral cortex estimated by intrinsic functional connectivity. J. Neurophysiol. 106, 1125–1165.

Zald, D.H., McHugo, M., Ray, K.L., Glahn, D.C., Eickhoff, S.B., Laird, A.R., 2014. Meta-analytic connectivity modeling reveals differential functional connectivity of the medial and lateral orbitofrontal cortex. Cereb. Cortex 24, 232–248.

Zwicker, J.G., Missiuna, C., Harris, S.R., Boyd, L.A., 2011. Brain activation associated with motor skill and practice in children with developmental coordination disorder: an fMRI study. Int. J. Dev. Neurosci. 29 (2), 145–152.